AGU PUBLICATIONS

Tectonics

RESEARCH ARTICLE
10.1002/2017TC004790

Special Section:
Orogenic cycles: from field observations to global geodynamics

Key Points:
- The Jurassic Neo-Tethys ridge was N-S trending and spreading at 1–2 cm/yr causing the widespread formation of detachment faults
- In the Middle Jurassic a N-S trending subduction zone formed near and parallel to the Neo-Tethyan ridge forming the West Vardar Ophiolite
- In the Middle Jurassic a N-S trending subduction zone was present near and parallel to the Neo-Tethyan ridge forming the West Vardar Ophiolite

Supporting Information:
- Supporting Information S1
- Data Set S1

Correspondence to:
M. Maffione,
m.maffione@bham.ac.uk

Citation:
Maffione, M., & van Hinsbergen, D. J. J. (2018). Reconstructing plate boundaries in the Jurassic Neo-Tethys from the East and West Vardar Ophiolites (Greece and Serbia). *Tectonics*, *37*, 858–887. https://doi.org/10.1002/2017TC004790

Received 31 AUG 2017
Accepted 8 FEB 2018
Accepted article online 14 FEB 2018
Published online 12 MAR 2018

Reconstructing Plate Boundaries in the Jurassic Neo-Tethys From the East and West Vardar Ophiolites (Greece and Serbia)

Marco Maffione[1,2] and Douwe J. J. van Hinsbergen[1]

[1]Department of Earth Sciences, Utrecht University, Utrecht, The Netherlands, [2]School of Geography, Earth and Environmental Sciences, University of Birmingham, Birmingham, UK

Abstract Jurassic subduction initiation in the Neo-Tethys Ocean eventually led to the collision of the Adria-Africa and Eurasia continents and the formation of an ~6,000 km long Alpine orogen spanning from Iberia to Iran. Reconstructing the location and geometry of the plate boundaries of the now disappeared Neo-Tethys during the initial moments of its closure is instrumental to perform more realistic plate reconstructions of this region, of ancient ocean basins in general, and on the process of subduction initiation. Neo-Tethyan relics are preserved in an ophiolite belt distributed above the Dinaric-Hellenic fold-thrust belt. Here we provide the first quantitative constraints on the geometry of the spreading ridges and trenches active in the Jurassic Neo-Tethys using a paleomagnetically based net tectonic rotation analysis of sheeted dykes and dykes from the West and East Vardar Ophiolites of Serbia (Maljen and Ibar) and Greece (Othris, Pindos, Vourinos, and Guevgueli). Based on our results and existing geological evidence, we show that initial Middle Jurassic (~175 Ma) closure of the western Neo-Tethys was accommodated at a N-S trending, west dipping subduction zone initiated near and parallel to the spreading ridge. The West Vardar Ophiolites formed in the forearc parallel to this new trench. Simultaneously, the East Vardar Ophiolites formed above a second N-S to NW-SE trending subduction zone located close to the European passive margin. We tentatively propose that this second subduction zone had been active since at least the Middle Triassic, simultaneously accommodating the closure of the Paleo-Tethys and the back-arc opening of Neo-Tethys.

1. Introduction

Global plate kinematic reconstructions are classically based on marine magnetic anomalies and fracture zones in the modern ocean basins, as well as paleomagnetic, structural, stratigraphic, and paleontological data from continents (e.g., Torsvik & Cocks, 2017). Such reconstructions identify that in the geological past oceanic basins must have existed that have now been lost due to subduction. The location, nature, and orientation of plate boundaries in plate reconstructions are relatively well constrained in modern ocean basins, or within or along continents. However, reconstructing plate boundaries and their orientations within lost ocean basins is notoriously difficult, and as a result, the detail in global plate reconstructions decreases back in geological time (termed "world uncertainty" by Torsvik et al., 2010). Reconstructing plate boundaries in deep geological time is crucial to reduce such world uncertainty and shed new light on tectonic processes that are poorly constrained based on modern analogues (e.g., subduction initiation).

In some cases, relics of oceanic lithosphere from subducted oceans are preserved in the geological record as ophiolites. The age of the ophiolitic crust, which once formed at an oceanic spreading center, is commonly inferred from geochronological analyses of igneous rocks and biostratigraphic analysis of overlying deep-marine sediments (e.g., Dilek & Furnes, 2011). Many ophiolites contain sheeted dyke sections, which are classically thought to have intruded along and parallel to the spreading ridge axis (e.g., Anonymous, 1972). Paleomagnetic analysis of sheeted dyke sections then allows restoring the dykes, and by inference the ridge at which they accreted, back to their original orientation (e.g., Morris et al., 1998; Inwood et al., 2009; Maffione, Thieulot, et al., 2015; Maffione et al., 2017; Morris & Maffione, 2016; van Hinsbergen et al., 2016). Combined with the existing global plate reconstructions, placed in a paleomagnetic frame of reference, it is then possible to constrain the orientations and approximate locations of spreading axes within now-subducted ocean basins, decreasing world uncertainty. Moreover, the geochemical affinity of ophiolites (i.e., mid-ocean ridge (MOR), supra-subduction zone (SSZ), or back-arc basin (BAB)) provides key constraints on the geodynamic

setting in which they formed and is crucial to infer potentially associated intraoceanic subduction zones (e.g., Maffione et al., 2017).

Here we apply such analysis to restore intraoceanic plate boundaries within the Middle Jurassic Neo-Tethys Ocean that existed between Greater Adria (a major Gondwana-derived block from which most of the Apennines, Alps, Dinarides, Hellenides, and Anatolide-Tauride orogens was derived) and Europe in the present-day eastern Mediterranean region. Overlying both the now-deformed paleomargins of Greater Adria and Europe in the Balkan-Anatolian orogen are widespread ophiolites of Early to Middle Jurassic age. These ophiolites in many places contain sheeted dykes with a dominant SSZ affinity and are widely interpreted to have formed above a nascent intraoceanic subduction zone (or zones) within the Middle Jurassic Neo-Tethys (e.g., Bortolotti et al., 2013; Dilek & Furnes, 2011; Maffione, Thieulot, et al., 2015; Robertson, 2002). In addition, some ophiolite bodies (also) provide MOR or BAB geochemical signatures (see next section).

Previously, Maffione et al. (2013) and Maffione, Thieulot, et al. (2015) piloted a paleomagnetic restoration of the MOR and SSZ affinity Mirdita ophiolite of Albania that now overlies units derived from the former Greater Adriatic margin and showed that this ophiolite formed at a N-S striking ridge. Maffione, Thieulot, et al. (2015) suggested that the transition from MOR to SSZ affinity within the ophiolite may reflect the inception of subduction below and parallel to the Neo-Tethys ridge in the Middle Jurassic. Here we build on this study and perform new paleomagnetic analyses from ophiolite bodies of Serbia and Greece to restore the orientation of the spreading ridges at which they formed and, for units with a subduction affinity, infer the geometry and orientations of associated subduction zone(s). We use these results to reconstruct a kinematically feasible, data-constrained Middle Jurassic intraoceanic plate boundary geometry of the Mediterranean Neo-Tethys.

2. Geological Setting and the Concept of the Neo-Tethys Ocean

Prior to the opening of the Atlantic Ocean, since Jurassic time, modern continents were part of the supercontinent Pangea, which in its heart, separating Gondwana in the south from Laurasia in the north, must have hosted a vast oceanic domain known as Tethys. This Tethyan domain has now largely been lost to subduction, but relics of its ocean basins and intervening continental fragments are now found in the Alpine mountain belt of the Mediterranean region (Figure 1). This mountain belt hosts a series of suture zones—locations marked by ocean-derived rocks (deep-marine sediments and ophiolites) where oceans must have disappeared upon subduction—bounded by accretionary fold-thrust belts (e.g., the Alps, Dinarides, Hellenides, and Rhodopes) derived from deformation of the continental margins of southern Laurasia and northern Gondwana bounding the Tethys.

Detailed study of these suture zones and adjacent continent-derived sedimentary units in the Mediterranean region has led to the recognition that since the Early Triassic or perhaps even earlier in the Permian, a series of oceanic basins formed within the Tethyan realm, conceptually known as the Neo-Tethys Ocean (e.g., Schmid et al., 2008; Stampfli et al., 1991). In the eastern Mediterranean region, there were two major oceanic Neo-Tethyan basins, north and south of an extended continental region known as the Adria-Turkey plate (Stampfli et al., 1991) or "Greater Adria" (Gaina et al., 2013). Opening of these Neo-Tethyan basins occurred, while Gondwana and Laurasia were still both part of Pangea and did not significantly move relative to each other. The area gained by Neo-Tethys opening must thus have been balanced by the closure of a preexisting ocean between Gondwana and Laurasia—the Paleo-Tethys. Finding the Paleo-Tethyan suture in the eastern Mediterranean region is challenging, but fragments of a Paleozoic oceanic basin are found in the Pontides of northern Turkey (e.g., Topuz et al., 2017; Ustaömer & Robertson, 1993). This geological evidence led to the interpretation that the Neo-Tethys Ocean opened due to the fragmentation of the northern margin of Gondwana and the northward migration of a "Cimmerian" continental ribbon terrane above a southward dipping, northward retreating slab consuming the Paleo-Tethys (e.g., Dokuz et al., 2017; Şengör & Yilmaz, 1981). Separation of this Cimmerian ribbon terrane from Greater Adria, which in Turkey is represented by the Sakarya terrane, led to the opening of the northern strand of the Neo-Tethys, also known as the Meliata-Maliac-Vardar Ocean in the west Neo-Tethys (modern Balkans) (Schmid et al., 2008), and Izmir-Ankara Ocean farther to the east (modern Turkey) (Şengör & Yilmaz, 1981). A southern strand separated Greater Adria from Africa, and relics are still underlying the eastern Mediterranean Sea today. Estimates of the age of the Ionian Basin suggest a Triassic age (Speranza et al., 2012), although to the east also Carboniferous

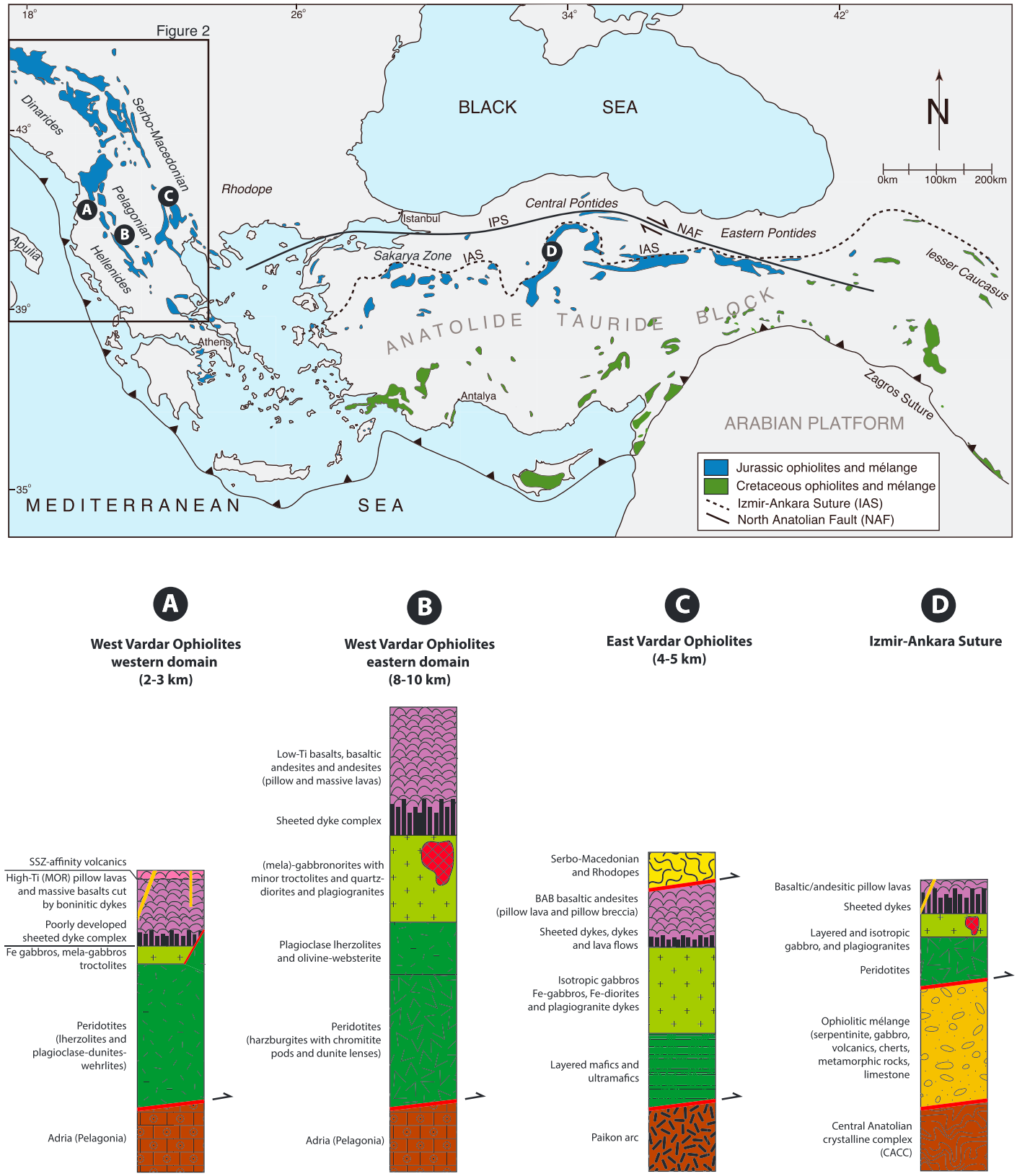

Figure 1. Distribution of the Jurassic (blue) and Cretaceous (green) ophiolites in the eastern Mediterranean region, and main geological domains and active faults. The Intra-Pontide suture (IPS) in the Central Pontides coincides with a segment of the North Anatolian Fault (NAF). Location of the representative summary stratigraphic logs for the four main ophiolite belts in the Balkan Peninsula and north Anatolia is indicated with letters A to D.

crust may be present, suggesting that northern Gondwana already had a complex paleogeography inherited from the Paleozoic (Granot, 2016). The collision of the Cimmerian ribbon with Eurasia, and the cessation of spreading of the Neo-Tethys Ocean, likely occurred in the Early to Middle Jurassic (Dokuz et al., 2017; Şengör & Yilmaz, 1981). Paleomagnetic data from the Pontides seem to confirm this hypothesis by showing that the Sakarya block was already part of Eurasia in the Middle Jurassic (Channell et al., 1996; Meijers et al., 2010).

Around the same time, the first known subduction-related geological records formed within the Neo-Tethyan basins in the form of SSZ ophiolites of Early to Middle Jurassic age. These ophiolites were emplaced onto the Eurasian and Greater Adriatic paleomargins and are now found in the Pannonian basin, the Dinarides, Albanides, Hellenides, and the Rhodopes, as well as in the Pontides and Izmir-Ankara suture zone of Turkey (e.g., Bortolotti et al., 2002; Bortolotti & Principi, 2005; Göncüoglu et al., 2012, 2014; Hoeck et al., 2009; Maffione, Thieulot, et al., 2015; Robertson, 2002, 2012; Schmid et al., 2008; Topuz et al., 2014; Ustaömer & Robertson, 1999) (Figure 1). These earliest Neo-Tethyan subduction zones in the central and eastern Mediterranean region formed contemporaneously with, and may have been caused by, the opening of the Central Atlantic Ocean that since ~175–170 Ma propagated as the Alpine Tethys into the western Mediterranean region separating Greater Adria from Iberia and Europe (e.g., Gaina et al., 2013; Labails et al., 2010; Maffione, Thieulot, et al., 2015; Stampfli et al., 1991; Vissers et al., 2013, 2017). These earliest, Jurassic subduction zones are no longer active today but terminated in the Early Cretaceous to Paleogene (e.g., Gürer et al., 2016; Schmid et al., 2008; Şengör & Yilmaz, 1981), after which ongoing Africa-Europe plate convergence became associated with formation of new subduction zones that led to complete closure of the Neo-Tethyan and Alpine Tethyan realms (e.g., Gaina et al., 2013; Maffione et al., 2017; Schmid et al., 2008; Stampfli et al., 1991).

The ophiolites from the Balkan Peninsula, exposed along a continuous NW-SE tending belt from the Dinarides to the Hellenides (Figure 2), contain well-exposed sheeted dyke sections and have been studied extensively in the last four decades providing an excellent basis to reconstruct intraoceanic plate boundaries in the western Neo-Tethys. The Dinaric-Hellenic fold-thrust belt is a ~1,000 km long orogenic belt running throughout the western part of the Balkan Peninsula (Figure 2) that formed during upper crustal accretion of subducting Greater Adriatic lithosphere (e.g., Dimitrijević, 1997; Schmid et al., 2008). This orogen is structured into a west verging imbricate stack of tectonic units derived from and emplaced onto the Adriatic passive margin since the Cretaceous. In the east, this belt is overthrust by the Datca and Circum-Rhodope megaunits (e.g., Schmid et al., 2008; Zelic et al., 2010).

Large, dismembered ophiolite bodies overlie both the Dinaric-Hellenic as well as the Datca and Circum-Rhodope fold-thrust belts (e.g., Bortolotti et al., 2013; Bortolotti & Principi, 2005; Robertson, 2002, 2012; Schmid et al., 2008). These ophiolites are subdivided into two belts: the western part of this ophiolite belt here called West Vardar Ophiolites following Schmid et al. (2008) (previously known as the Dinaric and Mirdita-Pindos ophiolites or the "West Vardar Zone ophiolites" (Bazylev et al., 2009; Hoeck et al., 2002; Karamata, 2006; Pamić et al., 1998, 2002; Robertson & Karamata, 1994; Smith & Spray, 1984)) is emplaced above Adria-derived units; the eastern part of this ophiolite belt here referred to as East Vardar Ophiolites following Schmid et al. (2008) (previously known as "Main Vardar Zone" ophiolite (e.g., Karamata, 2006) or "East Vardar Zone" ophiolite (Šarić et al., 2009)) is found above Europe-derived rocks (Schmid et al., 2008).

The West Vardar Ophiolites show a distinct west to east change of geochemical composition and internal structure (Figures 1 and 2). The western part of the West Vardar Ophiolites is dominated by fertile lherzolites, locally exposed in fossil oceanic core complexes (Maffione et al., 2013; Nicolas et al., 1999; Tremblay et al., 2009), and a thin crust with high-Ti MOR-affinity (Dilek et al., 2008; Saccani & Photiades, 2004). The high Ti/V ratios of these MOR-type ophiolites (e.g., Mirdita, Othris, and Pindos), ranging between 20 and 50, are incompatible with a subduction affinity (Reagan et al., 2010; Shervais, 1982) and strongly suggest that these MOR-type ophiolites represent relics of Neo-Tethyan lithosphere formed prior to subduction initiation (Maffione, Thieulot, et al., 2015). In places, for example in the Othris ophiolite (Figure 2) the West Vardar Ophiolites contain a diverse suite of mantle rocks, ranging from fertile lherzolites to depleted harzburgites, indicative of both anhydrous MOR-type and hydrous SSZ-type melting regimes (Barth et al., 2008). Also, the crustal section, besides the more typical MOR affinity, locally exhibits island arc tholeiite (IAT) and boninitic composition (Barth & Gluhak, 2009; Jones & Robertson, 1991; Photiades et al., 2003; Saccani & Photiades,

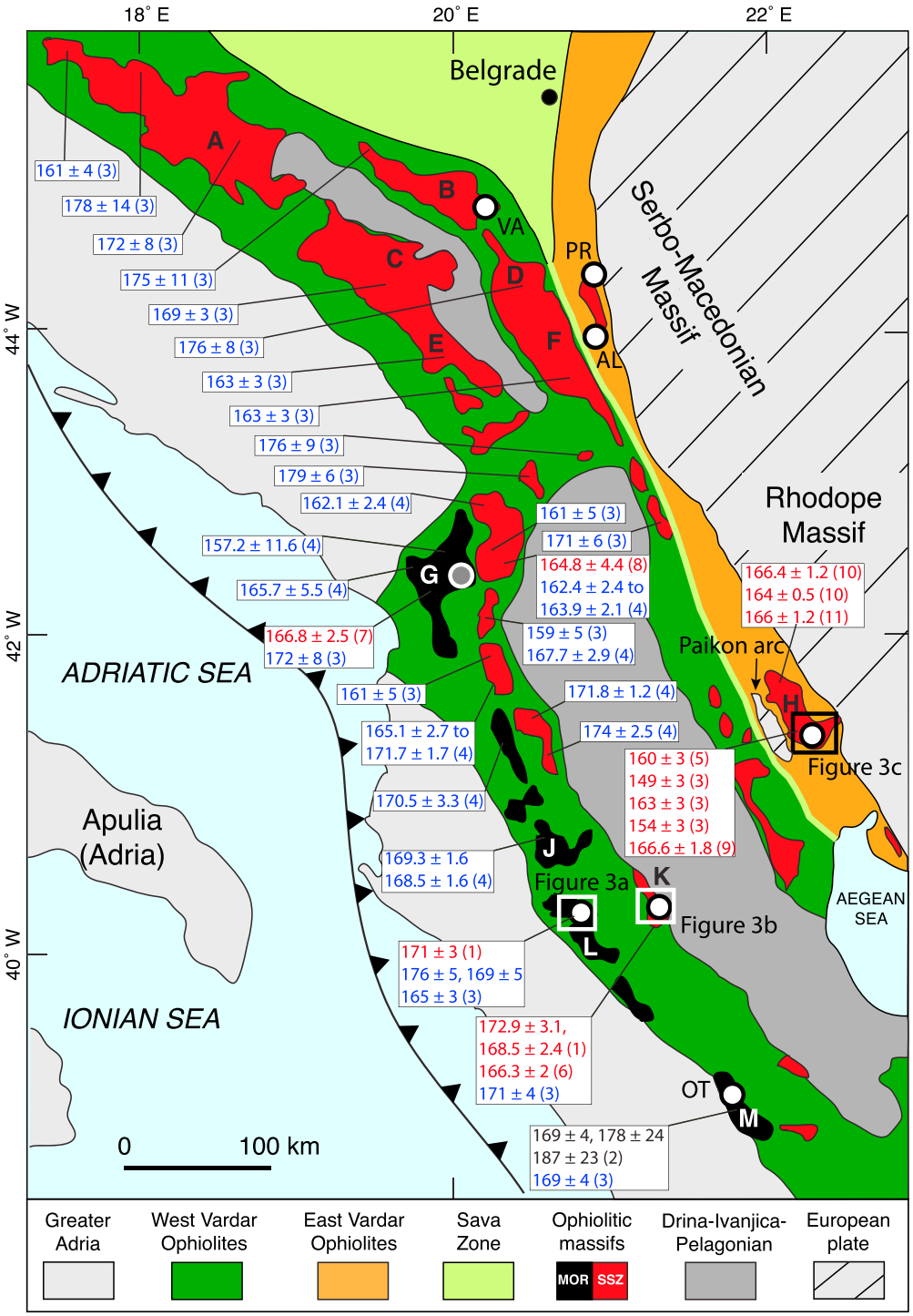

Figure 2. Simplified geological map of the central-western Balkan Peninsula showing the distribution the Jurassic ophiolites and the main geologic domains. The Sava zone (light green color) is the suture zone between the upper plate Tisza and Dacia Mega-Units and the lower plate internal Dinarides according to Schmid et al. (2008). The various ophiolite bodies are labeled as follows: A = Krivaja-Konjuh; B = Maljen; C = Zlatibor; D = Troglav; E = Bistrica; F = Ibar; G = north Mirdita; H = Guevgueli (south) and Demir-Kapija (north); J = south Mirdita; K = Vourinos; L = Pindos; and M = Othris. White dots indicate the sampling sites, which are labeled according to Table 1. Gray dot is the site in the Mirdita ophiolite studied by Maffione et al. (2013) and Maffione, Thieulot, et al. (2015). Specific location of the sites sampled in the Pindos, Othris, Vourinos, and Guevgueli ophiolites is shown in Figure 3. Ages (in Ma) of the ophiolitic crust (red) and subophiolitic metamorphic sole (blue) are shown in rectangles, with corresponding references indicated with number in brackets: (1) Liati et al. (2004) (U/Pb); (2) Ferriére (1982); (3) Spray et al. (1984) (Ar/Ar); (4) Dimo-Lahitte et al. (2001) (Ar/Ar); (5) Danelian et al. (1996) (radiolarian cherts); (6) Chiari et al. (2003) (radiolarian cherts); (7) Prela et al. (2000) (radiolarian cherts); (8) Marcucci et al. (1994) and Chiari et al. (1994) (radiolarian cherts); (9) Zachariadis (2007) (U/Pb); (10) Božović et al. (2013) (U/Pb and Ar/Ar); (11) Kukoč et al. (2015) (radiolarian cherts).

2004). These variations were interpreted by Maffione, Thieulot, et al. (2015) as the result of SSZ melts that during subduction initiation impregnated the preexisting Neo-Tethyan lithosphere formed at a MOR (termed "mantle refertilization" by Dijkstra et al., 2001). The eastern part of the West Vardar Ophiolites is dominated by depleted to ultradepleted harzburgites and a thick crustal sequence with a clear SSZ signature indicating formation above an active intraoceanic subduction zone (e.g., Pearce et al., 1984).

Crustal ages of the West Vardar Ophiolites span the latest Bajocian-early Oxfordian (~160–170 Ma) interval based on radiolarian cherts intercalated within the extrusive sequence of the Albanian Mirdita ophiolite (Chiari et al., 1994; Marcucci et al., 1994; Marcucci & Prela, 1996; Prela et al., 2000) and the Vourinos ophiolite of Greece (Chiari et al., 2003) (Figure 2). This age is comparable to zircon U-Pb ages of plagiogranites and gabbros from the Vourinos (172.9 ± 3.1 and 168.5 ± 2.4 Ma) and Pindos (171 ± 3 Ma) ophiolites (Liati et al., 2004) (Figure 2). Metamorphic soles are widespread below the West Vardar Ophiolites and show overall $^{40}Ar/^{39}Ar$ cooling ages of ~170 Ma (Dimo-Lahitte et al., 2001; Roddick et al., 1979; Spray & Roddick, 1980; Spray et al., 1984; Sostarić et al., 2014) (Figure 2). Because the cooling ages in metamorphic soles (probably slightly) postdate the actual inception of the subduction (van Hinsbergen et al., 2015), the data from Albania and Greece suggest that subduction in the western Neo-Tethys initiated in the Middle Jurassic, sometimes between 175 and 170 Ma.

The East Vardar Ophiolites are more dismembered and much less studied than the West Vardar Ophiolites. Crustal ages of the East Vardar Ophiolites are constrained only at the Guevgueli and Demir-Kapija ophiolite in northern Greece and southern Macedonia, respectively. In the Guevgueli ophiolite, radiolarian cherts intercalated with the extrusive sequence have been dated at 160 ± 3 Ma (Danelian et al., 1996). $^{40}Ar/^{39}Ar$ ages of gabbros and plagiogranites from the Guevgueli ophiolite vary between 149 ± 3 and 163 ± 3 Ma (Spray et al., 1984), while U/Pb dating of gabbros pinpoint the formation of the crust at 166.6 ± 1.8 Ma (Zachariadis, 2007). U/Pb ages of gabbro from the Demir-Kapija ophiolite in Macedonia range between 166.4 ± 1.2 and 164 ± 0.5 (Božović et al., 2013). This age is consistent with the late Bathonian-early Callovian (166 ± 1.2 Ma) radiolarian chert age determined by Kukoč et al. (2015), but is much older than the chert of the Guevgueli ophiolite studied by Danelian et al. (1996).

No metamorphic sole has been identified below the East Vardar Ophiolites. The geochemical composition of the East Vardar Ophiolites varies from BAB affinity in the south (Guevueli ophiolite; Saccani et al., 2008), to a mix of MOR- and SSZ-affinity that also includes boninites in Serbia and Macedonia (Božović et al., 2013; Marroni et al., 2004; Resimić-Šarić et al., 2005, 2006; Šarić et al., 2009). In northern Greece (Guevgueli ophiolite) the East Vardar Ophiolites occur between the deformed European margin (Rhodope Massif) and a continental fragment (i.e., Paikon arc; Brown & Robertson, 2004), which detached from either the continental margin of Europe (Anders et al., 2005; Brown & Robertson, 2004) or Greater Adria (Godfriaux & Ricou, 1991; Ricou & Godfriaux, 1991, 1995), and is intruded by the Fanos granite (158 ± 1 Ma; Anders et al., 2005). In Serbia the East Vardar Ophiolites, close to the Ibar ophiolite, are locally intruded by a quartzdiorite with U/Pb age of 168.4 ± 6.7 (Resimić-Šarić et al., 2005).

The origin of the Balkan ophiolites has long been debated, with different models suggesting their formation at one, two, or multiple oceans (for a review see Bortolotti et al., 2013). Most of the models invoking the existence of multiple oceans relied on the occurrence of large continental blocks (i.e., Drina-Ivanjica, Jadar, Kopaonik, and Pelagonian) in the West Vardar Ophiolites. According to the "multiple-ocean model," these continental blocks are interpreted as continental ribbons that separated discrete ocean basins in which individual ophiolite belts were created (e.g., Robertson & Karamata, 1994; Karamata, 2006). However, the West Vardar Ophiolites show a mainly westward emplacement direction, as indicated by the shear senses from the metamorphic sole of the Albanian ophiolites (Bortolotti et al., 2005; Carosi et al., 1996; Gaggero et al., 2009), and the structural polarity of emplacement-related deformation in the underlying fold-thrust belt (Tremblay et al., 2015). Given these constraints, we follow a more likely "single ocean model," which considers the continent-derived nappes exposed below the West Vardar Ophiolites as accreted parts of the now-subducted extended Greater Adriatic passive margin underlying an originally continuous ophiolitic nappe formed in a single ocean, that is, the western Neo-Tethys (Bernoulli & Laubscher, 1972; Bortolotti & Principi, 2005; Bortolotti et al., 2002, 2005, 2013; Chiari et al., 2011; Pamić et al., 1998; Schmid et al., 2008). Furthermore, the overall westward sense of emplacement of the West Vardar Ophiolites is seen as evidence that the associated initial subduction zone was dipping toward Europe (e.g., Bortolotti et al., 2013;

Maffione, Thieulot, et al., 2015; Schmid et al., 2008). Subsequent emplacement of the West Vardar Ophiolites occurred when the Adriatic margin entered the subduction zone in the latest Jurassic to Early Cretaceous (e.g., Schmid et al., 2008).

The East Vardar Ophiolites were thrust in Late Jurassic time upon units thought to belong to the former northeastern European margin of the Neo-Tethys, as suggested by Late Jurassic reef limestones uncomformably covering these ophiolites (Karamata, 2006; Schmid et al., 2008). The tectonic history that led to the formation and emplacement of the East Vardar Ophiolites is still controversial. Schmid et al. (2008) suggested that they formed upon Adria-ward, intraoceanic subduction in the Late Jurassic, followed by their obduction onto the Eurasian margin. In general, the East Vardar Ophiolites are thought to have formed close to or within the passive margin of Eurasia (ensialic marginal basin) upon back-arc extension produced by a Europe-dipping subduction zone (Bébien & Mercier, 1977; Bébien et al., 1987; Brown & Robertson, 2004; Robertson et al., 1996; Saccani et al., 2008; Zachariadou & Dimitriadis, 1995). To explain the emplacement of these ophiolites onto the Eurasian margin, Gallhofer et al. (2017) invoked a subduction polarity reversal (from Europe-ward to Adria-ward) occurring shortly after back-arc spreading of the Guevgueli basin. The long-term subduction evolution that led to the formation and emplacement of the East Vardar Ophiolites requires an in-depth analysis of the underlying orogen and is beyond the scope of this paper. Our results, however, will provide geometrical constraints on the orientation of the spreading centers and trenches (to the east or west of the ophiolite belt) in the Late Jurassic, which will help to formulate an alternative, geodynamically feasible model for the evolution of the East Vardar Ophiolites.

Jurassic ophiolites in Anatolia (Turkey) are exposed along two suture zones: the Intra-Pontide suture to the northwest, which separates the Eurasian Istanbul-Zonguldak terrane from the Sakarya terrane in the central Pontides, and the Izmir-Ankara suture zone to the south of the Pontides, which separates the Sakarya terrane from the Anatolide-Tauride belt (Figure 1) (see Göncüoglu et al., 2012, for an exhaustive review).

The Intra-Pontide suture (e.g., Şengör & Yilmaz, 1981) contains mainly Middle Jurassic ophiolites with MOR, SSZ, and BAB signatures (Göncüoglu et al., 2012; Ustaömer & Robertson, 1999), an ophiolitic mélange composed of ophiolitic fragments with both SSZ and BAB signatures, cherts with a Middle Triassic to Late Cretaceous age within a sedimentary matrix (Göncüoglu et al., 2014), and relics of an Upper Jurassic to Late Cretaceous high-pressure metamorphic accretionary complex (Marroni et al., 2014; Okay et al., 2013).

The Izmir-Ankara suture, to the south of the Sakarya terrane, contains an ophiolitic mélange and dismembered ophiolites (mainly composed of mantle units) with a variable geochemical signature ranging from MOR to BAB, IAT and boninitic (Bortolotti et al., 2017; Çelik et al., 2013, 2016; Parlak et al., 2013) (Figure 1). Crustal ages are scattered but cluster around 185–180 Ma (Dilek & Thy, 2006; Robertson et al., 2013; Uysal et al., 2015; Topuz et al., 2014), and associated metamorphic soles have slightly younger $^{40}Ar/^{39}Ar$ ages of 177.1 ± 1.0 and 166.9 ± 1.1 Ma (Çelik et al., 2011, 2013; Çörtük et al., 2016). South of the Izmir-Ankara suture, Upper Cretaceous ophiolites occur scattered above the Anatolide-Tauride belt (e.g., Maffione et al., 2017; Parlak, 2016; Robertson, 2002; Robertson et al., 2013) (Figure 1). No Jurassic ophiolites have been found underlying the Cretaceous ophiolites in Turkey and were thus not obducted onto Greater Adria prior to the Cretaceous. Therefore, the Jurassic ophiolites of the Izmir-Ankara suture are interpreted to have formed in the forearc south of the Sakarya terrane above a north dipping subduction zone consuming Neo-Tethyan lithosphere (Topuz et al., 2013, 2014).

3. Sampling and Methods

3.1. Study Areas

A regionally extensive paleomagnetic sampling was carried out from sheeted dyke sections of Serbia (Maljen and Ibar ophiolites) and Greece (Othris, Pindos, Vourinos, and Geuvgueli ophiolites), and discrete dykes intruding these ophiolites at different levels (Figure 2). Between 20 and 22 cylindrical oriented paleomagnetic cores were collected at each site in Serbia (63 cores in total) using a portable petrol-powered rock drill. A total of 257 paleomagnetic cores were obtained by subsampling hand samples (three to six at each site) collected from the ophiolites in Greece. At three sites of Greece (OT, Pi01, and Pi02) paleomagnetic cores were drilled in the field. Samples were collected in dykes showing doleritic composition and magmatic texture, and a low degree of weathering and alteration. Discrete dykes exposed within a few tens of meters were combined

into a single site. Dyke orientations were measured in the field only where chilled margins were observed. The orientation of at least ten adjacent dykes was measured at each site to calculate a statistically meaningful mean direction.

3.1.1. Maljen and Ibar Ophiolites (Serbia)

In Serbia we sampled sheeted dykes at three sections, one in the West Vardar Ophiolites near the village of Valjevo (VA, Maljen ophiolite) and two in the East Vardar Ophiolites near the village of Aleksandrovac (AL, Ibar ophiolite) and Prevest (PR, Ibar ophiolite) (Figure 2). Site AL corresponds to the site studied by Marroni et al. (2004), where boninitic dykes were documented. All samples were collected at abandoned quarries. Dykes at all sites are 1–1.5 mthick, doleritic in composition, and with clear chilled margins.

3.1.2. Pindos Ophiolite (Greece)

The Pindos ophiolite (Figure 2) is found over an imbricated stack of west verging thrust sheets of the Pindos nappe (unrelated to the ophiolite), composed of mixed pelagic and turbiditic sediments, platform carbonates, and mélange units overlying a Maastrichtian-Eocene flysch (Jones & Robertson, 1991; Saccani & Photiades, 2004). The ophiolite is composed of a lherzolitic mantle section (Dramala Complex), a metamorphic sole unit (Loumnitsa Unit), and a dismembered complex that includes layered ultramafic and mafic cumulates, isotropic mafic intrusive, sheeted dykes, and mafic extrusive rocks (Aspropotamos Complex) (Jones & Robertson, 1991; Montigny et al., 1973). The Pindos ophiolite is underlain by Upper Jurassic to Upper Cretaceous turbiditic carbonates and terrigenous sediments and Eocene-Miocene molasse deposits of the Meso-Hellenic trough (Jones & Robertson, 1991). The extrusive section shows a progressive variation from high-Ti affinity (lower lavas) derived from partial melting of a fertile mantle source, to very low Ti (boninitic) affinity (upper lavas and dykes) associated with partial melting of an ultradepleted mantle source (Saccani & Photiades, 2004).

Paleomagnetic sites in the Pindos ophiolite are mainly distributed along its eastern edge (Figure 3a). Sheeted dykes are not extensively exposed and were sampled only at one site (Pi05–08), while <1 m thick discrete dykes are abundantly exposed and were collected at three sites where they intrude peridotites (Pi01), gabbros (Pi02–04), and lavas (Pi10). Pillow lavas were observed at a few tens of meters from site Pi05–08, and their bedding was measured to provide paleohorizontal constraints for the rotation analysis.

3.1.3. Othris Ophiolite (Grece)

The Othris ophiolite in southern mainland Greece is located in the MOR-affinity domain of the West Vardar Ophiolites and is a lateral equivalent of the Pindos ophiolite (Figure 2). This ophiolite is highly dismembered, with the different units being tectonically juxtaposed in reverse order, from bottom to top: cherts and pillow lavas, sheeted dykes and gabbro cumulates, ultramafic cumulates, and tectonic slices of mantle rocks (Barth et al., 2008; Barth & Gluhak, 2009). Exposures of the sheeted dykes are very limited and not always easy to recognize in the field. Here we sampled a set of adjacent 0.5–1 m thick doleritic dykes with chilled margins at one site (OT) corresponding to site M3 of Barth and Gluhak (2009), which corresponds to dolerites with an E-MORB affinity (Figure 3b).

3.1.4. Vourinos Ophiolite (Greece)

The Vourinos ophiolite is located ~50 km to the east of the Pindos ophiolite within the SSZ-affinity domain of the West Vardar Ophiolites (Figure 2). Although mantle rocks predominate, the Vourinos ophiolite shows a Penrose-type pseudostratigraphy composed of a 7 km thick harzburgitic mantle sequence overlain by a 3–4 km thick crustal sequence including layered gabbro, sheeted dykes, and basaltic to andesitic lavas (e.g., Moores, 1969; Rassios, 1981). The extrusive sequence displays both IAT (Krapa Hill series) and boninitic composition (Asprokambos series) (Beccaluva et al., 1984), and the mantle section is ultradepleted (Kapsiotis, 2014), showing the SSZ affinity of the ophiolite.

Our study area in the Vourinos ophiolite is the Krapa Hills section where a continuous sequence from mantle rocks to the extrusive sequence is exposed (Figure 3c). Here the ophiolite is strongly tilted to the WSW, resulting in exposure of mantle units to the east and crustal rocks to the west (Rassios & Dilek, 2009). Sheeted dykes were sampled at one site (VO01–05), while gabbro-hosted ~1.5 m thick discrete dykes were sampled at two additional sites (VO06 and VO07).

3.1.5. Guevgueli Ophiolite (Greece)

The Guevgueli ophiolite (Figure 2) is divided into a west and east Guevgueli subunit (Bébien, 1977), with the Fanos granite (158 ± 1 Ma; Anders et al., 2005) occurring in the middle (Christofides et al., 1990; Soldatos et al., 1993). In both domains, the ophiolitic sequence contains a thick crustal sequence that includes cumulates

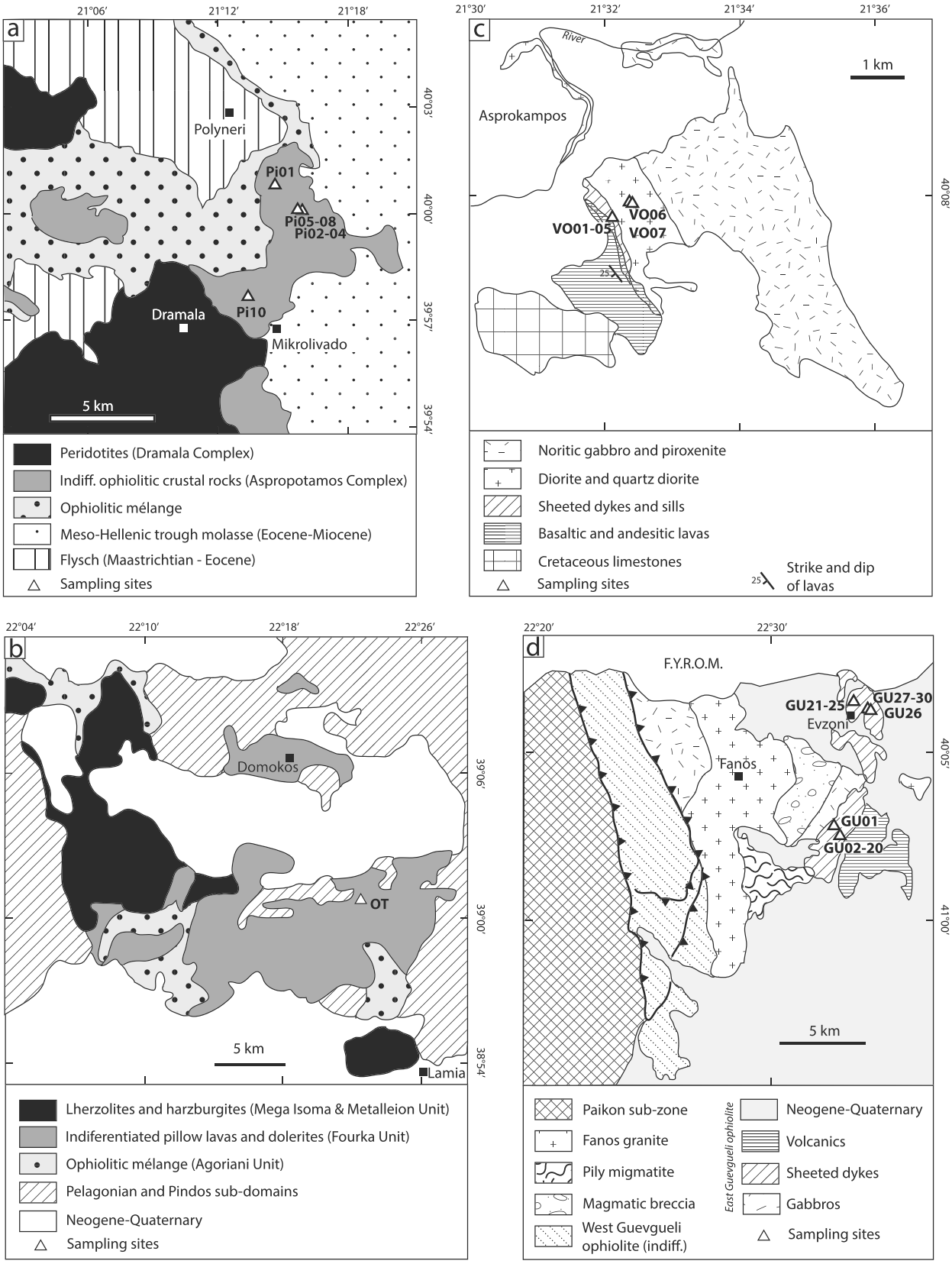

Figure 3. Simplified geological maps of the (a) Pindos, (b) Othris, (c) Vourinos, and (d) Guevgueli ophiolites, redrawn after Saccani and Photiades (2004), Bortolotti et al. (2008), Moores (1969), and Saccani et al. (2008), respectively.

and isotropic gabbro, sheeted dykes with a basaltic to dacitic composition, and basaltic lavas (Robertson, 2002). Sampling in the Guevgueli ophiolite was carried out at five localities from the East Guevgueli subunit (Figure 3d). Well-exposed sheeted dykes showing chilled margins (except site GU27–30) were sampled at four sites, while discrete dykes in gabbros were sampled at one site (GU01).

3.2. Paleomagnetism, Rock Magnetism, and Petrography

Characteristic remanent magnetizations (ChRMs) were isolated using alternating field (AF) demagnetization treatment up to 100 mT. Approximately 20% of the samples from Greece (twin specimens) were also demagnetized thermally up to 580°C or until complete demagnetization. Demagnetization experiments were carried out in the magnetically shielded room of the "Fort Hoofddijk" paleomagnetic laboratory (Utrecht University) using a robotized cryogenic magnetometer (2G Enterprise). Demagnetization data were plotted on orthogonal diagrams (Zijderveld, 1967), and remanence components were isolated via principal component analysis (Kirschvink, 1980) using online software www.paleomagnetism.org (Koymans et al., 2016). Isolated ChRMs with maximum angle of deviation (Kirschvink, 1980) larger than 15° were discarded. Site mean directions were computed using Fisherian statistics (Fisher, 1953) on virtual geomagnetic poles correspondent to the isolated ChRMs after applying a fixed 45° cutoff (Johnson et al., 2008) to the obtained data set. Quality criteria of Deenen et al. (2011) were adopted to assess whether paleosecular variation (PSV) of the geomagnetic field is adequately represented within the samples collected at each site (i.e., $A_{95min} < A_{95} < A_{95max}$). Underrepresentation of PSV (i.e., $A_{95} < A_{95min}$) in dykes may indicate either rapid cooling or remagnetization, while overrepresentation of PSV (i.e., $A_{95} > A_{95max}$) denotes the occurrence of additional sources of scatter in addition to PSV, for example, within-site deformation or an inefficient preservation of the remanence.

The nature, grain size, and distribution of the magnetic carriers were determined in representative samples by (i) investigating the blocking temperatures during thermal variation (20–700°C, in five heating–cooling subcycles with increasing peak temperature) of low-field magnetic susceptibility experiments using a KLY-3 Kappabridge coupled with a CS3 apparatus, (ii) determining hysteresis parameters with a Princeton AGM Micromag magnetometer and using them to build Day plots (Day et al., 1977), and (iii) carrying out microscopic observations on polished thin sections with both a transmitted light microscope and a scanning electron (JEOL JCM-6000) microscope (SEM) coupled with an energy-dispersive X-ray (EDX) analyzer for elemental analysis.

3.3. Net Tectonic Rotation Analysis

The primary goal of the net tectonic rotation analysis is to determine the geometry of the spreading systems at which the Balkan ophiolites formed, and from here to infer the configuration of the Neo-Tethyan ridges or subduction zone(s) that initiated within the Neo-Tethys in the Middle Jurassic. Sheeted dyke complexes in ophiolites are composed of multiple intrusions of vertical dykes, which emplaced along a spreading axis. The initial (predeformation) direction of dykes from a sheeted dyke complex therefore indicates the orientation of the spreading ridge at which an ophiolite was formed (e.g., Anonymous, 1972; Maffione, Thieulot, et al., 2015; Maffione et al., 2017). On the other hand, discrete dykes crosscutting ophiolites at any level do not necessarily intrude vertically and parallel to the suprasubduction spreading ridge; yet they may still provide important information on the regional stress field affecting the overriding plate during ongoing subduction, assuming that they intrude along fractures formed roughly perpendicularly to the main stretching direction.

The effect of local deformation needs to be removed from sheeted dykes and discrete dykes to determine their initial orientation. Classical "tilt correction" used in paleomagnetic studies to calculate local deformation is, however, not applicable to dykes where paleohorizontal controls are typically not available, and tilt does not necessary occur along dyke-parallel axes (as required for the tilt correction approach). Tilting a vertical dyke along a horizontal axis not parallel to the dyke strike can in fact produce an apparent rotation component about a vertical axis that cannot be removed or identified using classical tilt correction approach. This implies that the initial dyke orientation cannot be obtained by simply removing the tilt and restoring the dyke to vertical (an approach widely used in the past).

Several studies have shown, especially in units lacking paleohorizontal control like dykes in ophiolites, that the most reliable approach for rotation analysis is a net tectonic rotation analysis (Hurst et al., 1992; Inwood et al., 2009; Maffione, Thieulot, et al., 2015; Maffione et al., 2017; Morris & Anderson, 2002; Morris

et al., 1998, 1990, 2002; Morris & Maffione, 2016; van Hinsbergen et al., 2016). This method, originally devised by Allerton and Vine (1987), rather than decomposing the deformation into a tilt and a vertical-axis component, calculates the single rotation that restores the sampled rock unit to its original (vertical or horizontal) position, and simultaneously the measured in situ remanence to its initial predeformation direction.

The initial reference direction, called "reference magnetization vector"—RMV, can be identified based on the expected direction from a stable plate at a given time. In this way, deformation is calculated with respect to the stable plate. In this study, we analyze the rotation in an absolute reference frame, that is, relative to the geographic north, because ophiolites form originally as independent intraoceanic microplates before being emplaced on a specific continental margin. This makes it difficult to select a specific reference stable plate for ophiolites. The net rotation calculated using an absolute reference frame, therefore, includes any combination of plate motion and intraplate local deformation. The RMV used in our analysis has declination (D) of 360° or 180°, depending on whether the polarity of the geomagnetic field was normal or reverse at the time of remanence acquisition. The RMV inclination (I) is chosen based on the expected paleolatitude of the ophiolite. Because we make no a priori assumption on the paleolatitude of the studied ophiolites, we assume their initial location as spanning the maximum latitudinal extent of the western Neo-Tethys Ocean in the Middle Jurassic. Paleogeographic reconstruction at 170 Ma placed in a paleomagnetic reference frame (Torsvik et al., 2012) indicates that the southern margin of Eurasia and the northern margin of Gondwana (at the approximate location where the studied ophiolites were emplaced) were located at 35°N and 15°N, respectively. The corresponding inclination and associated error of the magnetic field expected for this latitude range is $I = 41.3° \pm 13.2°$. In our analysis we therefore use two RMVs for each site, one for a normal polarity field case ($D/I = 000°/41.3°$), and one for a reverse polarity field case ($D/I = 180°/-41.3°$).

A set of net tectonic rotation solutions is expressed as the azimuth and plunge of the rotation axis, magnitude and sense of rotation, and initial orientation of the paleosurface. When applied to dykes, two sets of solutions are obtained if they are restored to vertical. In this case, three selection criteria are used to determine the preferred solution at each site: (1) the rotation parameters should be able to reproduce the local tilt inferred from the distribution of the different ophiolitic subunits at the study area (assuming the boundaries between subunits—e.g., mantle-crust or gabbro-sheeted dykes—as originally horizontal); (2) the kinematics of the preferred solution (e.g., sense and magnitude of rotation) have to be consistent with the known regional and/or local deformation pattern; (3) if multiple sites within a relatively small region are sampled, the preferred net tectonic rotation parameters should be consistent across the study area (assuming local rotations to be trivial).

On the other hand, single solutions are obtained when dykes cannot be restored to vertical (e.g., because they did not intrude vertically). Single solutions are geologically meaningless as both the initial dyke orientation and the rotation parameters strictly depend on the orientation of the chosen RMV.

Once a preferred solution has been chosen, an iterative net tectonic rotation analysis is then applied to model the uncertainties on the input vectors (RMV (only the inclination), site mean direction, and dyke orientation) following the method described by Morris et al. (1998) and modified by Koymans et al. (2016). This routine within the net tectonic rotation analysis package is available at www.paleomagnetism.org. Modeling of the errors produced between 75 (single solution) and 150 (dual solutions) permissible net tectonic rotation solutions at each site.

4. Results

4.1. Paleomagnetism

All samples from Serbia and Greece have a relatively weak magnetization ranging between 0.3 and 400 mAm^{-1}; yet about 90% of the samples yield a stable and measurable remanence. Two components of magnetization are commonly observed: a low-stability component, which was removed at 5–10 mT or 150–200°C, and a ChRM component, which was isolated at 70–100 mT or 560–580°C (Figure 4). Medium destructive fields (i.e., the alternating magnetic field necessary to remove half of the natural remanent magnetization) are variable between 5 and 50 mT. AF demagnetization curves are generally straight or concave upward. AF demagnetization treatment was more effective than thermal cleaning, the latter mainly producing noisy Zijderveld diagrams. Thermal treatment was effective only on samples

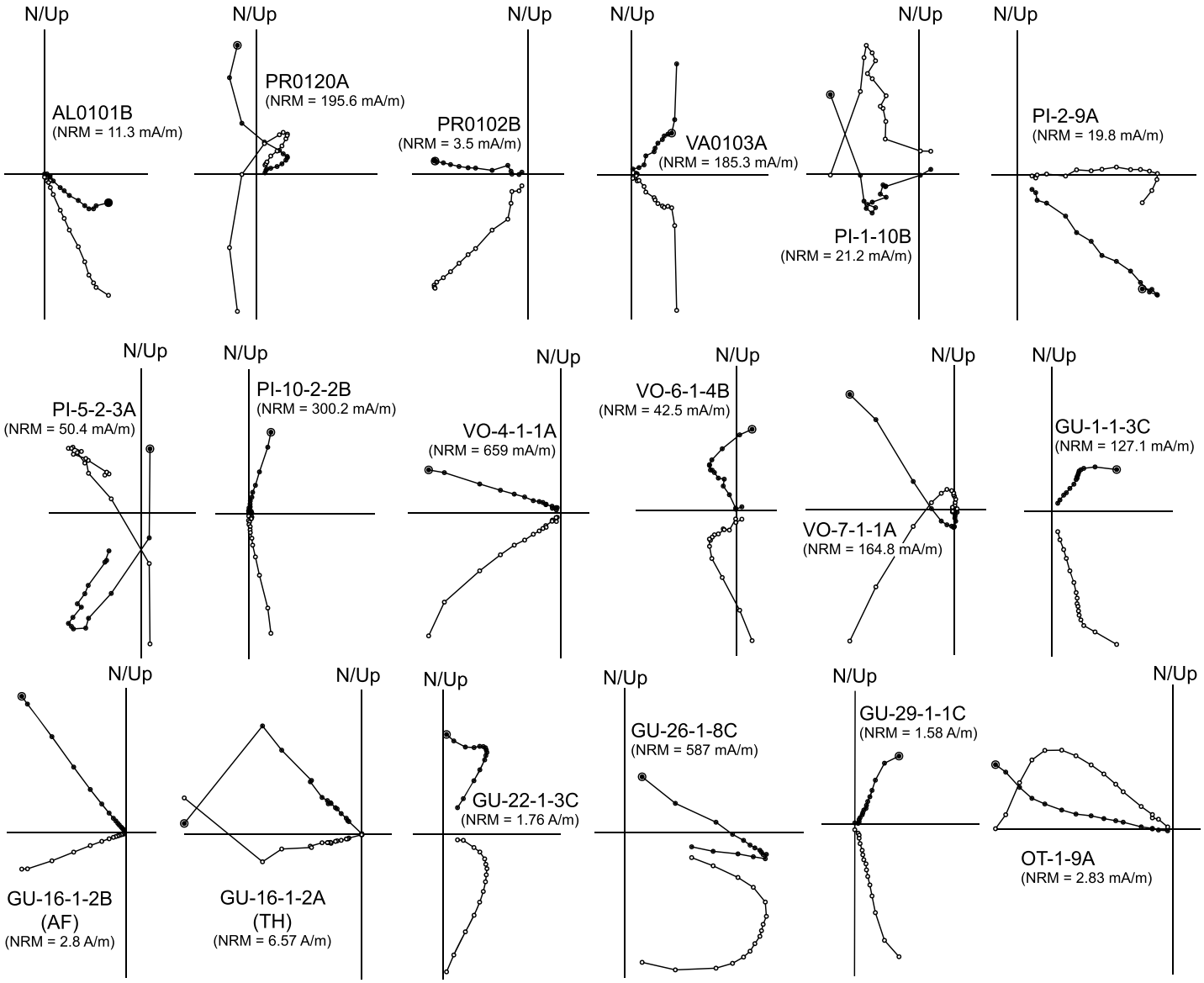

Figure 4. Zijderveld diagrams (Zijderveld, 1967) of representative samples demagnetized using thermal (TH) and alternating field (AF) treatment, shown in in situ coordinates. Solid and open dots represent projections on the horizontal and vertical planes, respectively. Demagnetization step values are in °C or in mT.

from Guevgueli (Greece), where the results obtained from AF and thermal demagnetizations of twin specimens are comparable (Figure 4).

PSV is adequately sampled at all sites ($A_{95min} < A_{95} < A_{95max}$), except GU02–20 where even after the 45° cut-off has discarded about half of the samples the A_{95} value remains slightly larger than that expected from PSV (Table 1 and Figure S1 in the supporting information). All computed in situ site mean directions (Table 1 and Figure S1) are significantly different from the present-day geocentric axial dipole field (D/I = 000°/59.1° in Greece, and D/I = 000°/62.6° in Serbia), excluding recent remagnetization. Only at site Pi10 from the Pindos ophiolite the calculated mean direction is within error from the present-day field, indicating possible recent remagnetization. ChRMs from all sampled sites are provided in the supporting information in a ".pmag" format compatible with the http://paleomagnetism.org software.

4.2. Rock Magnetism and Microscope Observations

Ratios of hysteresis parameters (Mrs/Ms, Hcr/Hc) for representative samples were plotted on a Day plot (Day et al., 1977) to determine the gran size of the magnetic carriers (Figure 5a). Data fall between the

Table 1
Paleomagnetic Results From the West and East Vardar Ophiolites of Serbia and Greece

Site	Ophiolite	Lithology	Latitude	Longitude	Dip dir./Dip	N	N_{45}	D	dD	I	dI	k	α_{95}	K	A_{95}	A_{95min}	A_{95max}
							Serbia										
AL	Ibar	Sheeted dykes	43.465670	20.933930	214/87	20	19	144.1	8.1	59.0	5.6	38.8	5.5	29.8	6.3	3.7	12.8
PR	Ibar	Sheeted dykes	43.759058	21.031641	137/84	14	12	039.2	8.1	−55.3	6.5	69.3	5.3	44.3	6.6	4.4	17.1
VA	Maljen	Sheeted dykes	44.107298	19.901759	048/32	22	18	028.8	10.3	48.4	10.4	28.2	7.9	15.8	9.0	3.8	13.3
							Greece										
Pi01	Pindos	Dyke in peridotite	40.013056	21.244667	178/68	16	15	246.4	18.9	−67.6	8.6	24.5	7.9	11.2	11.9	4.1	14.9
Pi02–04	Pindos	Dyke in gabbro	40.000222	21.259444	300/71	34	28	176.0	8.7	−9.8	16.9	9.0	9.7	10.9	8.7	3.2	10.0
Pi05–08	Pindos	Sheeted dykes	40.000389	21.257861	308/35	16	9	210.7	10.3	−10.1	20.0	16.5	13.1	26.2	10.3	5.0	20.5
Pi10[a]	Pindos	Dyke in basalt	39.963833	21.221083	190/75	6	4	008.5	31.7	57.3	23.0	29.8	17.1	15.0	24.5	6.9	34.2
OT	Othris	Sheeted dykes	39.011333	22.377194	098/18	25	18	283.7	10.9	−40.1	13.9	13.5	9.8	12.8	10.1	3.8	13.3
VO01–05	Vourinos	Sheeted dykes	40.125273	21.534818	244/38	21	17	286.4	10.3	26.9	16.8	9.8	12.0	13.9	9.9	3.9	13.8
VO06	Vourinos	Dyke in gabbro	40.128888	21.540832	202/63	10	10	338.1	9.3	40.0	11.8	30.9	8.8	32.8	8.6	4.8	19.2
VO07	Vourinos	Dyke in gabbro	40.128889	21.540833	088/80	6	5	201.3	21.6	−46.2	23.2	24.1	15.9	17.1	19.1	6.3	29.7
GU01	Guevgueli	Dyke	41.058333	22.553889	241/68	6	6	050.2	26.5	63.6	15.6	29.1	12.6	12.6	19.6	5.9	26.5
GU02–20	Guevgueli	Sheeted dykes	41.047306	22.564444	299/77	63	35	070.8	12.5	56.8	9.4	8.4	8.9	7.0	9.9	2.9	8.7
GU21–25	Guevgueli	Sheeted dykes	41.109333	22.558972	116/52	20	16	002.8	10.2	29.8	16.0	9.3	12.8	15.1	9.8	4.0	14.3
GU26	Guevgueli	Sheeted dykes	41.108000	22.562528	152/15	17	16	118.2	6.1	9.6	12.0	19.7	8.5	37.3	6.1	4.0	14.3
GU27–30	Guevgueli	Sheeted dykes	41.108520	22.562864	100/24	17	16	045.4	10.6	62.0	6.4	51.7	5.2	24.1	7.7	4.0	14.3

Note. Dyke orientation is expressed as dip direction/dip. N = total number of processed specimens; N_{45} = number of specimens used for the calculation of the mean values after filtering with a 45° cutoff (Johnson et al., 2008). D, dD = site mean declination and associated error; I, dI = site mean inclination and associated error; k and α_{95} = precision parameter and semiangle of the 95% cone of confidence around the computed site mean direction; K and A_{95} = precision parameter and semiangle of the 95% cone of confidence around the mean virtual geomagnetic pole; A_{95max} and A_{95min} = maximum and minimum value of A_{95} expected from paleosecular variation of the geomagnetic field calculated after Deenen et al. (2011).
[a]Discarded site due to possible remagnetization.

two theoretical mixing curves between single domain (SD) and multidomain (MD), and SD and superparamagnetic (SP) (Dunlop, 2002). This indicates the occurrence of mixtures of SD, MD, and SP grains, with a predominance of MD grains (generally >50%). In detail, samples from the Pindos ophiolite are the ones showing the largest grain size of magnetite with >90% of MD grains, while samples from site PR in Serbia shows the smallest grain fraction with about 50% of MD grains. SP grains seem to be present in all samples, with the larger content observed at the Othris ophiolite (OT).

Thermal variation of the low-field magnetic susceptibility of all samples shows a rapid decay between 500 and 580°C (Figures 5b and 5c), consistent with the presence of magnetic fractions with Curie temperatures close to that of nearly stoichiometric magnetite or low-Ti titanomagnetite (Dunlop & Özdemir, 1997). Increase of susceptibility between 100 and 250°C followed by a progressive decrease between 250 and 400°C was observed during heating cycles, likely due to production of low-Ti titanomagnetite or maghemite upon oxidation during heating under natural oxidizing conditions (no argon gas was used for the experiments). However, it cannot be excluded that a small fraction of these two minerals was originally present in the analyzed samples. Some samples from the Pindos and Othris ophiolite yielded noisy demagnetization diagrams characterized by an overall progressive decay of the magnetic susceptibility, indicating a predominance of the paramagnetic over the ferromagnetic fraction.

Isotropic fabric and moderate to pervasive weathering characterize all thin sections analyzed under the transmitted light microscope (Figure S2). The studied rocks are composed of an assemblage of plagioclase (~50–80%), chlorite and prehnite (~20–40%), clinopyroxene (~5%), and opaque minerals (~5%). Most of clinopyroxene minerals are pervasively or entirely altered into chlorite, as indicated by the occurrence of several chlorite pseudomorphs. Opaque minerals are distributed randomly within the mineral matrix.

SEM observations coupled with EDX analysis indicated the occurrence of stoichiometric magnetite and low-Ti titanomagnetite (Figure S3). Presence of small euhedral iron sulfides growing along the edges of titanomagnetite crystals has been observed in a sample from the Othris ophiolite. SEM observations evidenced the occurrence of large MD magnetite grains ranging between 50 and 150 μm, as well as SD to PSD grains smaller than 3 μm.

In summary, results from the rock magnetics experiments, EDX analysis, and optical observations of polished thin sections indicate that the magnetic remanence of the studied rocks is carried by a mixture of SP, SD, and

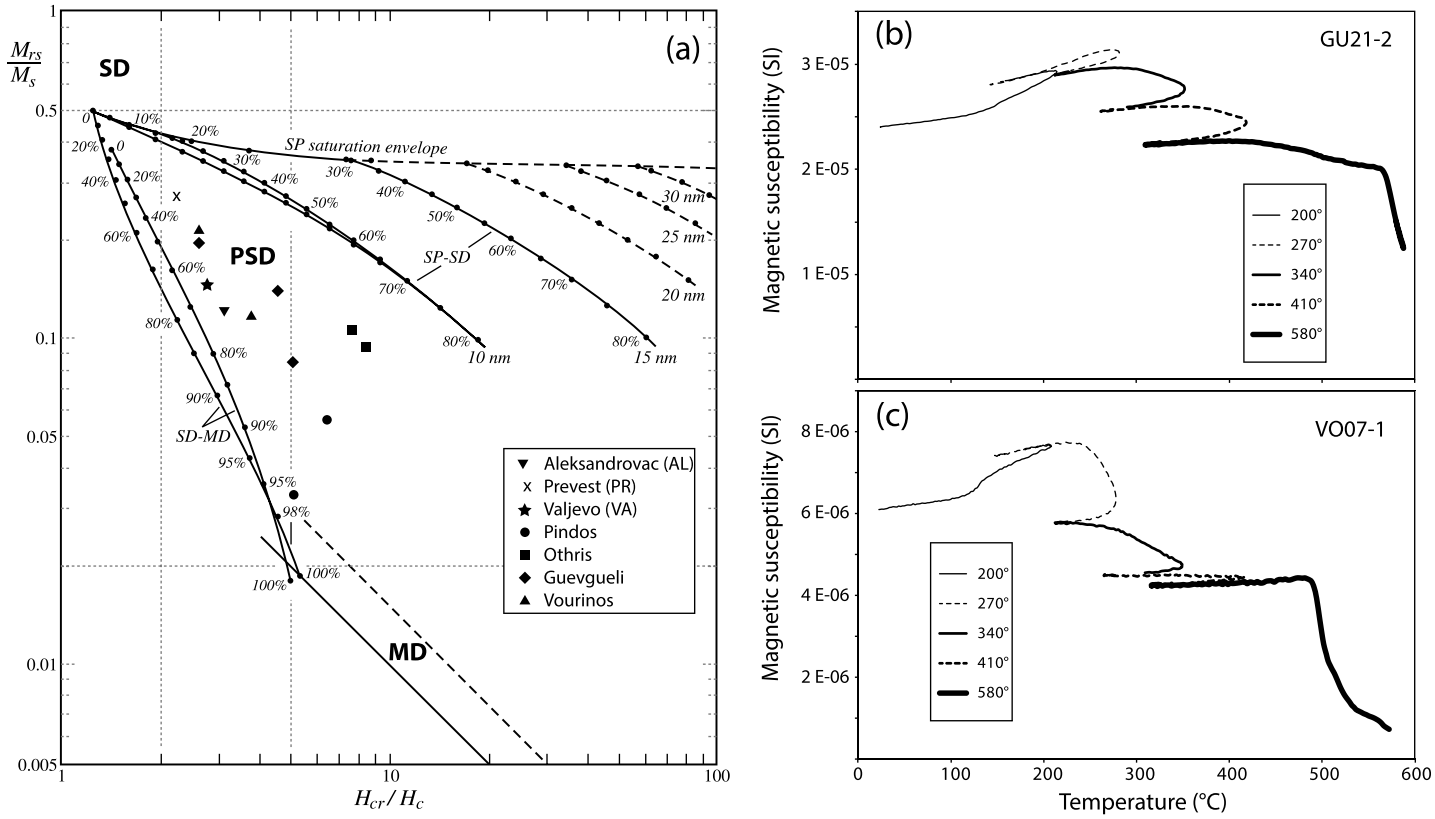

Figure 5. (a) Day plot (Day et al., 1977) for representative samples, showing the theoretical mixing curves for SD-MD grains (left), and SD-SP grains (right). Data fall in the PSD field of the diagram, between the SD-MD and the 10 nm SD-SP mixing curves, hence showing the occurrence of a mixed fraction containing SP, SD, MD grains. (b, c) Thermal variation of the low-field magnetic susceptibility for two representative samples from the (b) Guevgueli and (c) Vourinos ophiolite. Experiments were run under free air. Each curve consists of a combination of five heating-cooling subcycles, with increasing peak temperatures (shown in the enclosed rectangle) up to 580°C. Every subcycle consisted in heating up to a chosen peak values followed by cooling at a temperature higher than the value. Both diagrams show two blocking temperature ranges, the first at 200–410°C and the other at ~580°C.

MD grains of magnetite and minor titanomagnetite of magmatic origin. All rocks show an isotropic doleritic texture and a mineralogical assemblage compatible with a low greenschist metamorphic facies, which likely resulted from static seafloor hydrothermal alteration. Despite this mild metamorphism, which may have partially overprinted primary magnetizations, the isolated ChRMs were very likely recorded during or shortly after dyke intrusion (hence parallel to the primary magnetization).

4.3. Net Tectonic Rotation Analysis

Four sets of net tectonic rotation solutions (two for each reference direction used) were obtained at all sites except VO06, where single solutions (per reference direction) were obtained (Table 2). Although the net tectonic rotation analysis calculates the rotation around an inclined axis, it is always possible to infer, based on the plunge of the rotation pole, the relative magnitude of tilt and vertical axis rotation component. Tilt or vertical-axis rotation components are larger when the rotation pole is shallower or more steeply plunging, respectively. The magnitude of resulting tilt and vertical-axis components were considered in this study to select the preferred net tectonic rotation solutions, based on the criteria presented in the method section (Table 2). In particular, those solutions producing extreme tilting (up to overturning, which is rarely observed in the Neo-Tethyan ophiolites) or very large vertical axis rotation incompatible with the expected regional pattern have been discarded.

4.3.1. Maljen and Ibar Ophiolites (Serbia)

No major regional vertical axis rotations affected the Dinaridic nappes since their Cretaceous accretion, and declinations from Cretaceous rocks of the Dinarides tend to show small counterclockwise rotations resulting from their motion together with Adria (e.g., Márton et al., 2010). Ophiolites overlying these units do not

Table 2
Results of the Net Tectonic Rotation Analysis Showing the Four Permissible Solutions Obtained at Each Site by Using Both Normal (N) and Reversed (R) Polarity Reference Direction

		Solution 1					Solution 2				
		Rotation axis		Rotation			Rotation axis		Rotation		
Site	Ref. dir.	Azimuth	Plunge	Magnitude	Sense	Initial dyke strike	Azimuth	Plunge	Magnitude	Sense	Initial dyke strike
					Serbia						
AL	N	068.9	35.0	99.7	CCW	010.1	318.0	79.6	135.3	CW	349.9
AL	R	**235.7**	**16.1**	**108.5**	**CCW**	**349.9**	157.3	7.2	167.1	CW	010.1
PR	N	**115.8**	**17.2**	**103.2**	**CW**	**359.3**	203.5	5.4	168.9	CCW	000.7
PR	R	290.4	26.1	95.2	CW	000.7	045.8	81.5	135.5	CCW	359.3
VA	N	**018.9**	**32.8**	**77.6**	**CCW**	**023.7**	011.3	49.7	138.0	CW	336.3
VA	R	246.4	30.4	160.3	CCW	336.3	153.3	36.6	166.4	CCW	023.7
					Greece (Pindos)						
Pi01	N	116.1	3.0	152.8	CW	320.7	236.6	26.5	137.3	CCW	039.3
Pi01	R	**282.2**	**60.5**	**58.6**	**CW**	**039.3**	041.3	39.7	91.7	CCW	320.7
Pi02–04	N	**277.4**	**53.5**	**162.3**	**CW**	**038.3**	088.0	0.6	148.5	CCW	321.7
Pi02–04	R	349.1	26.2	128.9	CCW	321.7	267.8	6.9	31.7	CCW	038.3
PI05–08	N	119.6	22.8	139.9	CCW	005.5	242.4	54.8	168.3	CCW	354.5
Pi05–08	R	**043.2**	**40.5**	**82.5**	**CW**	**354.4**	007.1	17.9	118.9	CCW	005.5
					Greece (Othris)						
OT	N	277.4	27.0	120.9	CCW	329.9	184.3	25.6	121.4	CCW	030.1
OT	R	**231.3**	**8.9**	**79.5**	**CW**	**030.1**	052.4	51.8	173.2	CCW	329.9
					Greece (Vourinos)						
VO01–05	N	157.1	31.4	63.0	CCW	003.7	317.4	45.6	161.0	CCW	356.3
VO01–05	R	**072.3**	**24.6**	**160.0**	**CW**	**356.3**	193.2	35.1	124.3	CW	003.7
VO06[a]	N	350.0	29.5	71.3	CW	090.0	—	—	—	—	—
VO06[a]	R	**107.1**	**28.4**	**170.5**	**CW**	**090.0**	—	—	—	—	—
VO07	N	168.6	43.7	166.5	CCW	348.9	274.9	5.4	173.0	CCW	011.1
VO07	R	**009.7**	**45.4**	**163.5**	**CW**	**011.1**	212.8	37.0	16.2	CW	348.9
					Greece (Guevgueli)						
GU01	N	**334.8**	**67.5**	**78.7**	**CW**	**080.3**	295.8	65.2	55.0	CW	279.7
GU01	R	127.1	12.8	168.1	CW	279.7	115.3	4.9	159.9	CW	080.3
GU02–20	N	**316.6**	**77.1**	**75.8**	**CW**	**313.6**	028.0	56.0	172.8	CW	046.4
GU02–20	R	127.2	5.7	169.2	CW	046.4	175.6	30.7	149.6	CCW	313.6
GU21–25	N	350.6	33.3	65.2	CCW	050.0	000.8	35.4	167.9	CCW	310.0
GU21–25	R	**250.7**	**26.4**	**171.6**	**CW**	**310.0**	190.3	54.1	178.8	CCW	050.0
GU26[b]	N	219.0	39.0	104.0	CW	356.1	074.4	45.9	173.4	CW	003.9
GU26[b]	R	308.9	31.0	134.8	CCW	003.9	175.4	14.5	96.1	CCW	356.1
GU27–30[b]	N	032.0	38.9	89.4	CCW	067.9	022.1	49.9	148.7	CCW	292.1
GU27–30[b]	R	238.2	29.0	146.3	CCW	292.1	200.1	36.2	153.0	CCW	067.9

Note. The preferred solutions are in bold character. Sense of rotation is clockwise (CW) or counterclockwise (CCW).
[a]A single solution was obtained at this site indicating that dykes could not be restored to vertical (see text). [b]No preferred solution could be chosen at this site.

necessarily reflect their deformation pattern due to the possibility of intraoceanic rotations. Paleomagnetic data from the volcanic units of the Mirdita ophiolite of Albania (Maffione et al., 2013), however, indicate only a minor clockwise (CW) net rotation of that portion of the ophiolite belt, which is consistent with the regional rotation pattern of the subophiolitic continental units (e.g., Márton et al., 2010). We therefore used this evidence as a guide to selecting the preferred net tectonic rotation solutions, whereby small vertical axis rotation components are thus more likely than large rotations (the latter would require major intraoceanic rotations of the ophiolite). All results from Solution 2 (Table 2) from the three sites studied in Serbia were discarded as they produce either nearly complete overturning of the units or large vertical axis rotation components incompatible with the regional rotation pattern. At each site, out of the two available results from Solution 1 we selected the one yielding the smallest magnitude of vertical axis rotation component, that is, those with the shallowest rotation axis or lowest rotation amount or a combination of the two (Table 2). The preferred solutions produce moderate tilting of the ophiolite and minor, both CW and counterclockwise (CCW), vertical axis rotation, which altogether suggest no significant rotation of the studied area consistently with the regional rotation pattern.

The restored initial strike of the sheeted dykes from Serbia varies around a N-S direction (Table 2). More precisely, modeling of the uncertainties in the net tectonic rotation analysis following the method of Morris et al.

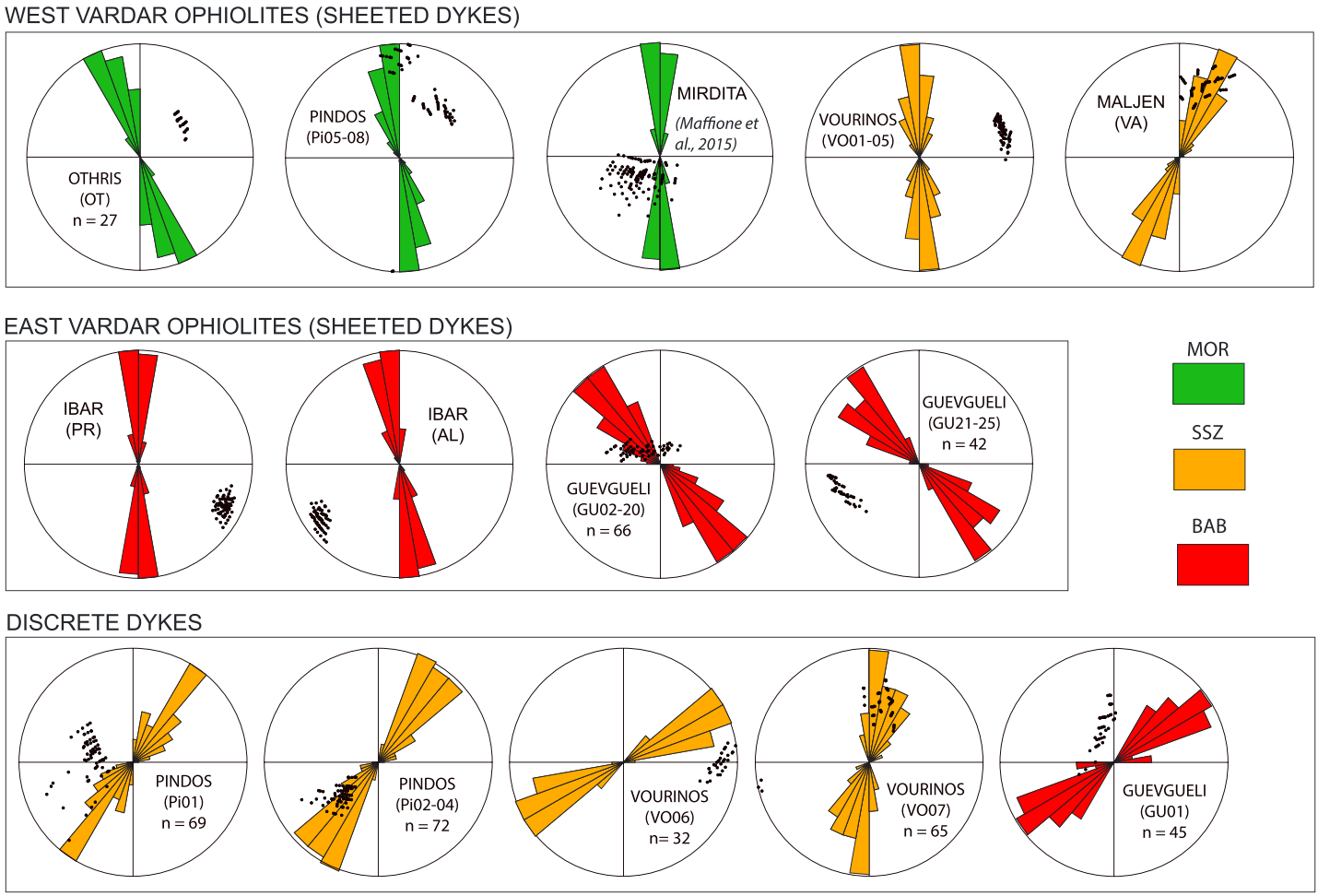

Figure 6. Rose diagrams showing the preferred initial orientations (strike) of the studied sheeted dykes and discrete dykes obtained after modeling of the uncertainties in the net tectonic rotation analysis (Allerton & Vine, 1987) following the methods of Morris et al. (1998) and subsequent modifications by Koymans et al. (2016). The restored directions of MORB sheeted dykes (green) provide the trend of the Neo-Tethyan ridge, while the restored directions of SSZ and BA sheeted dykes indicate the strike of the suprasubduction ridge at which the ophiolites were generated. Black dots are the calculated rotation axes after error modeling. All diagrams are based on 75 solutions (maximum number of solutions after each error modeling), except few sites in which a lower amount of solutions (*n*) has been obtained.

(1998) provided most frequent strike values between 350° and 360° (a 10° frequency interval was adopted throughout this study to build the frequency distribution diagrams of Figure 6) at sites AL and PR from the East Vardar Ophiolites, and between 020° and 030° at site VA in the West Vardar Ophiolites.

4.3.2. Othris Ophiolite

Net tectonic rotation analysis at site OT from the Othris ophiolite provided four solutions: three of which indicate large tilt and CCW vertical axis rotations, and one yields a moderate tilt and minor CW vertical axis rotation (Table 2). Pelagonian Upper Triassic to Upper Cretaceous carbonate units underlying the ophiolites of southern Greece show an overall CW rotation of ~94° (Morris, 1995). According to Morris (1995), such net rotation resulted from a Late Cretaceous-early Miocene CW rotation of ~50°, followed by a post middle Miocene CW rotation of additional ~45° associated with the bending of the Hellenic arc (e.g., van Hinsbergen et al., 2005; van Hinsbergen & Schmid, 2012).

While this regional rotation might not necessarily be reflected in the overlying Othris ophiolite because of possible intraoceanic rotations, it still represents a useful constraint for our net tectonic rotation analysis. In fact, since the large post-Late Cretaceous CW rotation of Greece has to contribute to the net rotation of the Othris ophiolite, the three permissible net tectonic rotation solutions indicating large CCW rotations (see Table 2) would require an unlikely extremely large (150–180°) preobduction CCW rotation of the ophiolite. On

the other hand, the remaining CW net tectonic rotation solution (Table 2) indicating moderate tilt and no significant vertical axis rotation components would instead require a smaller (~90°) and, therefore, geodynamically more feasible CW vertical axis rotation of the ophiolite before its obduction, a rotation that has been observed in other ophiolites, including the well-studied Troodos ophiolite of Cyprus (e.g., Morris & Maffione, 2016).

Furthermore, although the Othris ophiolite appears quite dismembered in the study area (Figure 3b) the southward transition from dolerites to pillow lavas documented by Barth and Gluhak (2009) in our study area would suggest a general southward tilt of the ophiolite. Modeling of the errors on the CW net tectonic rotation solution yielded two groups of solutions: 54 solutions indicating moderate (72°–96°) CW rotations about a shallow SW plunging axis and 27 solutions showing large (157°–179°) CW rotation about a steeper NE plunging axis. The latter set of solutions reproduces even better the regional post-Late Cretaceous rotation pattern of Greece, without the need for any intraoceanic rotation of the Othris ophiolite. Furthermore, this solution well reproduces the local deformation (i.e., southward tilt) observed at the sampling site and has therefore been chosen as preferred solution (Table 2). The initial dyke orientation for the preferred set of solutions indicate an average strike ranging between 330° and 340° (i.e., ~NNW-SSE; Figure 6).

4.3.3. Pindos Ophiolite

The local orientation of the Pindos ophiolite units in our sampling region is difficult to determine due to the predominant exposures of ultramafic rocks and the absence of visible subunit boundaries. Luckily, close to site Pi05–08 pillow lavas dipping 58° toward 180° occur, providing important paleohorizontal constraints for selecting the preferred net tectonic rotation solutions. A tilt-corrected direction of D = 239.2°, $I = -54.2°$ is obtained by correcting the in situ remanence of site Pi05–08 (Table 1) for the local tilt inferred from the pillow lavas. Such tilt corrected direction reveals a vertical axis CW rotation of 59.2°, which suggests substantial rotation of the Pindos ophiolite, consistent with the regional post-Late Cretaceous CW rotation in Greece (e.g., Morris, 1995). It is worth noting that tilt correction in pillow lavas may be biased by the fact that these units may be emplaced on paleoslopes (up to ~20° dip). However, while an uncertainty on the vertical axis rotation of site Pi05–08 inferred from the tilt-corrected direction of the nearby pillow lavas cannot be excluded, the possibility that the inferred CW sense of rotation may instead be CCW remains low. We therefore consider the CW sense of rotation calculated at site Pi05–08 using classic tilt correction of adjacent pillow lavas layering sufficiently reliable and used it for the selection of the preferred net tectonic rotation solution at the remaining sites of the Pindos ophiolite. Furthermore, similarly to the Othris ophiolite, a CW vertical axis rotation of the Pindos ophiolite would exclude any (unlikely) major intraoceanic rotations.

Only one out of four permissible net tectonic rotation solutions for sites Pi02–04 and Pi05–08 yield a CW rotation (hence chosen as preferred solution; see Table 2). These preferred solutions are characterized by a moderately dipping rotation axis and moderate to large rotations producing significant tilt and moderate (CW) vertical axis rotation components. The vertical axis rotation component appears to be substantially larger at site Pi02–04 possibly due to local rotations associated to an undetected fault. At the remaining site Pi01 two permissible solutions with CW rotation were obtained (Table 2). Only the one characterized by a steeper rotation pole, which produces a local rotation consistent with that inferred at sites Pi05–08 and Pi02–04, was selected as preferred solution.

Initial dyke orientation is indistinguishable for the two discrete dykes sites Pi01 and Pi02–04, where dykes were restored to an initial strike of ~040°, while it is substantially different at the sheeted dyke site Pi05–08, where dykes have an initial strike of 354.4° (Table 2). Modeling of the uncertainties on the input vectors of the preferred solutions yielded most frequent orientations between 020° and 040° (i.e., NE-SW) for the mantle- and gabbro-hosted discrete dykes and between 350° and 360° (i.e., N-S) for the sheeted dykes (Figure 6).

4.3.4. Vourinos Ophiolite

The Vourinos ophiolite is characterized by a locally vertical, NW-SE striking crustal-mantle boundary, with the crust and mantle sections exposed to the SW and NE, respectively, indicating an overall southwestward tilt of the ophiolite (Figure 3c). Four solutions were obtained at sites VO01–05 and VO07, while only two at site VO06 where dykes are restored to an initial dip of 87.1°, hence very close to vertical (Table 2).

At site VO01–05 only the result from Solution 1 indicating a CW rotation around a shallowly plunging axis (selected as preferred solution; Table 2) can replicate exactly the local structural setting and produce a

southwestward tilt and vertical strata. The discarded three solutions yield tilt to the NW, NE, and SE, which is inconsistent with that observed at this study area. Site VO06 only provided single solutions (one for each reference direction adopted; Table 2) and in theory should be discarded. However, because the single solution restored the dyke nearly to the vertical, error modeling may produce a variable number of dual solutions that may still be used for our analysis. Among the two single solutions (one per reference direction) obtained at site VO06, only the one with the larger rotation is able to replicate the local distribution of ophiolitic units. After having modeled the uncertainties on the input vectors for this single solution, dykes could be restored to vertical in 32 out of 75 iterations. These solutions indicate a large CW rotation about a shallowly plunging axis. At site VO07 both results from Solution 2 produce a northwestward tilt, which in one case produces overturning, inconsistent with the local structural pattern. Both Solution 1 result in vertical strata, but we chose as preferred solution the one characterized by a CW rotation (Table 2), as it is consistent with the regional rotation of the underlying Pelagonian units (Morris, 1995).

The initial dyke orientation of the sheeted dyke complex (preferred solution) of the Vourinos ophiolite (VO01–05) has a strike of 356.3° (Table 2), with most frequent values determined from error modeling between 350° and 360° (i.e., N-S; Figure 6). At site VO06 the gabbro-hosted dykes have a most frequent initial strike between 050° and 070° (i.e., ENE-WSW; Figure 6). Site VO07 has an initial dyke orientation of 011.1° (Table 2) with most frequent directions after error modeling between 000° and 010° (i.e., N-S; Figure 6).

4.3.5. Guevgueli Ophiolite

The Chalkidiki peninsula onto which the Guevgueli ophiolite was emplaced underwent some 30° CW rotation in the Neogene during opening of the Rhodope extensional complex (e.g., Brun & Sokoutis, 2007; Kondopoulou & Westphal, 1986; van Hinsbergen & Schmid, 2012), and prior to this time, Eurasia did not appreciably rotate since the Late Jurassic (Torsvik et al., 2012). Moderate CW rotations should thus be expected at this ophiolite if it did not experience any intraoceanic rotations, hypothesis that is not supported by direct evidence. For this reason, we only used the local deformation to select the preferred net tectonic rotation solutions. The Guevgueli ophiolite is locally characterized by an east-southeastward tilt, which causes the exposure of upper crustal units in the east and gabbros in the west. Preferred solutions reproducing both this local and regional deformation have been identified at sites GU01, GU02–20 and GU21–25 (Table 2). The discarded three solutions at each one of these sites produce in fact rotations that are clearly inconsistent with the local tilt of the ophiolite. At site GU21–25 the large rotation around a shallow axis indicates a larger tilt compared to sites GU01 and GU02–20, but virtually a similar and significant amount of CW vertical axis rotation component across the three sites.

No preferred solution could be found at the remaining two sites GU26 and GU27–30 as none of the obtained solutions could reproduce either the local deformation or the overall regional CW rotation. This may be caused by the occurrence of local rotations not recognized in the field, which make the choice of the preferred solution uncertain. We therefore prefer to exclude sites GU26 and GU27–30 from further analyses.

Modeling of uncertainties on the preferred solutions from the discrete dykes (GU01) and sheeted dykes (GU02–20 and GU21–25) indicates most frequent initial strike values between 050° and 060°, and between 310° and 330°, respectively (Figure 6).

5. Discussion: Plate Boundary Configuration of the Middle Jurassic Mediterranean Neotethys

5.1. Assumptions and Boundary Conditions

We now use our net tectonic rotation results, in combination with the previously reported geochemical signatures of the Balkan ophiolites, to infer a plate boundary configuration within the Middle Jurassic Neo-Tethys. We thereby assume that the MOR-type ophiolites from the western part of the West Vardar Ophiolite belt (western Mirdita, Othris, and Pindos ophiolites; Figure 2) are relics of Neo-Tethyan lithosphere formed at a MOR setting (Barth et al., 2008; Nicolas et al., 1999; Maffione, Thieulot, et al., 2015). We interpret ophiolites with a SSZ affinity as formed in a forearc close to a trench shortly after subduction initiation (e.g., Stern et al., 2012). The Guevgueli ophiolite (Figure 2), with a BAB geochemical signature, is interpreted to have formed in a back-arc position.

The orientation of the ridges at which SSZ ophiolites were formed may also be used to infer the geometry of the associated subduction zone (Maffione et al., 2017; van Hinsbergen et al., 2016). The angular relationship between a SSZ ridge and the associated trench may vary between two end-members: perpendicular or parallel to the associated subduction trench (e.g., Casey & Dewey, 1984; Dewey & Casey, 2013). The West Vardar Ophiolites presently form a ~100–150 km wide belt, which under typical magmatic spreading rates of 4 cm/yr or more would have formed within ~5 Ma if suprasubduction ridges were oriented parallel to the trench. Conversely, an ~1,000 km long ophiolite belt (like the West Vardar Ophiolites) formed at suprasubduction ridges perpendicular to the trench would display laterally diachronous ages spanning tens of millions of years. The consistent age of the SSZ West Vardar Ophiolites varying within no more than 10 Ma over a distance of several hundreds of kilometers along its length, thus strongly suggests that they formed at suprasubduction ridges that were parallel to the Neo-Tethyan subduction zone. In addition, as mentioned before, our reconstruction assumes that the East and West Vardar Ophiolites formed within a single ocean, which is the simplest explanation of the available data (Bernoulli & Laubscher, 1972; Bortolotti et al., 2002, 2013; Bortolotti & Principi, 2005; Gallhofer et al., 2017; Schmid et al., 2008; Tremblay et al., 2015).

Finally, net tectonic rotation results obtained from discrete dykes sampled at five sites from the Pindos, Vourinos, and Guevgueli ophiolites indicate a consistent ~NE-SW initial orientation at four out of five localities (Figure 6; Table 2). This direction is substantially different from the reconstructed initial orientation of the sheeted dykes from the correspondent ophiolite. This indicates that discrete dykes did not intrude parallel to the suprasubduction ridges at which the Balkan ophiolites were formed. Because of this, results from the discrete dykes have not been used to reconstruct the geometry of the plate boundaries in the western Neo-Tethys.

Although no ages are available for the sampled discrete dykes, their SSZ (Pindos and Vourinos) and BAB (Guevgueli) signatures (Figure 6), and their crosscutting relationship with the other units of the ophiolites they intrude indicate that they were emplaced after the formation of the ophiolitic crust (<165 Ma) but before their emplacement onto the Adriatic and Eurasian margins (>130 Ma). The consistent NE-SW orientation of these discrete dykes (Figure 6) may perhaps be indicative of a uniform, subduction-related extensional stress field directed roughly NW-SE and active between the Middle Jurassic and the Early Cretaceous.

5.2. West Vardar Ophiolites and Neo-Tethyan Ridge Inversion

Our results show that the sheeted dykes from the MOR-type ophiolites of the West Vardar belt (Othris and Pindos) formed along a ridge that seems to bend southward from a N-S to a NNW-SSE strike (Figure 6 and Table 2). Previous paleomagnetic results from the Mirdita ophiolite (Albania), ~300 km to the north, yielded a similar N-S paleoridge orientation (Maffione, Thieulot, et al., 2015). We follow previous inferences (Barth & Gluhak, 2009; Nicolas et al., 1999; Maffione, Thieulot, et al., 2015) arguing that these MOR-type ophiolites represent relics of crust that formed at the Neo-Tethyan mid-oceanic ridge prior to subduction initiation and conclude that the Neo-Tethys Ocean in the Middle Jurassic opened due to ~E-W spreading, at high angles to the European and Adriatic margins (Figure 7).

The SSZ-affinity sheeted dykes from more internal West Vardar Ophiolites (Vourinos and Maljen) were restored to a N-S to NNE-SSW orientation (Figure 6 and Table 2), indicating that also these ophiolites formed at approximately N-S striking ridges that accommodated E-W extension. As mentioned previously, the very similar, 170–160 Ma ages of the West Vardar Ophiolites along the Balkan-Hellenic orogen leads us to infer that the trench above which these ophiolites formed was parallel to these SSZ spreading ridges, that is, N-S striking. This inference is consistent with the top-to-the-west emplacement direction inferred from the metamorphic soles, and the near-synchronous Early Cretaceous emplacement age onto the Greater Adriatic margin (Bortolotti et al., 2005; Carosi et al., 1996; Gaggero et al., 2009; Scherreiks et al., 2014; Schmid et al., 2008).

Maffione, Thieulot, et al. (2015) suggested, based on the paleomagnetic restoration of the Mirdita ophiolite, that a N-S striking subduction zone formed parallel to the Neo-Tethys ridge. Based on the finding of an eastward dipping fossil oceanic detachment fault in the Mirdita ophiolite (Maffione et al., 2013; Maffione, Thieulot, et al., 2015), these authors showed that the new trench developed off-axis, to the west of the Neo-Tethyan ridge, west of the current MOR-affinity belt, likely by inversion of similar but slightly older oceanic detachment faults. Reactivation of the former Neo-Tethyan spreading center above the nascent

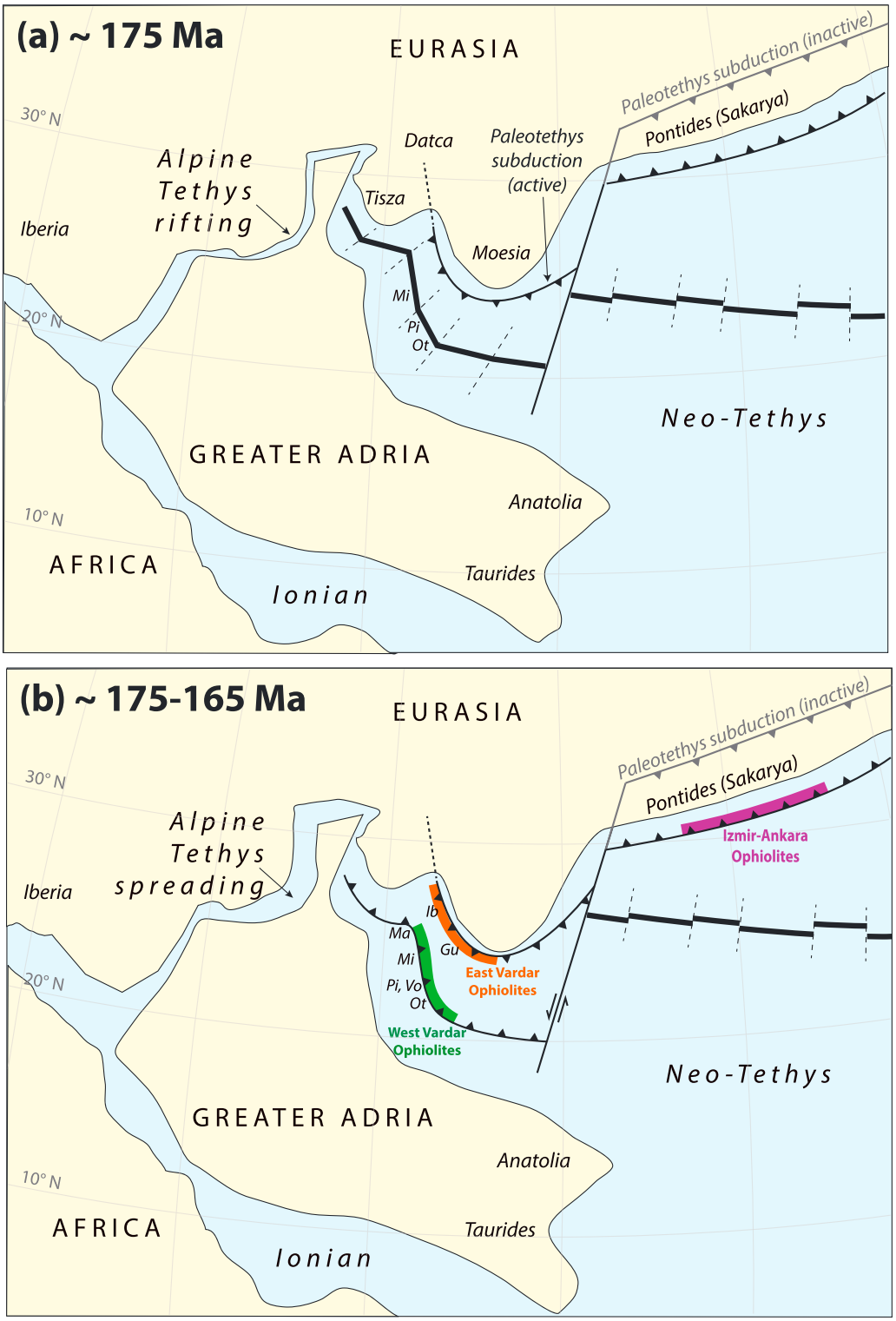

Figure 7. Paleogeographic reconstructions of the Neo-Tethys domain (a) before subduction initiation at ca. 175 Ma, and (b) shortly after between ca. 175 and 165 Ma. Position of the Eurasian, Adriatic, and African continental margins has been reconstructed using GPlate software and a paleomagnetic reference frame (Torsvik et al., 2012). Latitude is constrained with a ±3° uncertainty, while longitude is not constrained. Spreading ridges (thick black lines), transform faults (thin black line), and trenches (thin line with triangles) are shown. The location of the MOR ophiolites derived from the Neo-Tethys Ocean is shown in stage (a), while these plus the SSZ and BAB ophiolites produced after subduction initiation are shown in stage (b). The ophiolite codes are as follows: Ma = Maljen ophiolite; Ib = Ibar ophiolite; Mi = Mirdita ophiolite; Gu = Guevgueli ophiolite; Pi = Pindos ophiolite, Vo = Vourinos ophiolite, and Ot = Othris ophiolite. The locations of the West Vardar Ophiolite belt (green), East Vardar Ophiolite belt (orange), and Izmir-Ankara Ophiolite belt (purple) are indicated by the thick colored lines.

subduction zone then generated the SSZ ophiolites. Our new results from MOR and SSZ West Vardar Ophiolites show that this model may now be applied along the strike of the Mediterranean Neo-Tethys, from the northern Dinarides to the southern Hellenides (Figure 7).

That subduction initiation occurred along the Neo-Tethyan MOR was previously conceptually inferred based on the interpretation that metamorphic soles require abnormally high mantle temperatures, which are expected close to spreading centers (e.g., Bortolotti et al., 2002; Robertson, 2002; van Hinsbergen et al., 2015; Wakabayashi & Dilek, 2003). However, recent studies showed that several Cretaceous ophiolites of Turkey formed above a subduction zone that initiated along ancient N-S striking fracture zones (Maffione et al., 2017) and that the ophiolites of southern Tibet formed in the forearc of a subduction zone nucleated along a continental margin (Maffione, van Hinsbergen, et al., 2015; Huang et al., 2015). Both ophiolite belts are associated with in situ or dismembered metamorphic soles (e.g., Çelik et al., 2006; Guilmette et al., 2009), suggesting that metamorphic soles are not necessarily evidence for subduction initiation along ridges (Maffione et al., 2017). The long delay of ~30–40 Ma between subduction initiation (Middle Jurassic) and emplacement of the West Vardar Ophiolites on the continental margin (Early Cretaceous), however, is consistent with a subduction initiation far from the Greater Adriatic margin, hence close to the spreading ridge.

Applying the model of off-axis subduction initiation along detachments to the ~1,000 km long Neo-Tethyan ridge along the Balkan-Hellenic orogen would require the widespread presence of such detachments, which has only been documented in the Mirdita ophiolite (Maffione et al., 2013; Nicolas et al., 1999; Tremblay et al., 2009). That such detachments were likely widespread may, however, be inferred from kinematic calculations. Paleogeographic reconstructions of both the Paleo-Tethys (Franke et al., 2017) and Neo-Tethys (Schmid et al., 2008; Stampfli & Hochard, 2009; Gaina et al., 2013; Vissers et al., 2013) suggest that the Tethys Ocean in the study area was 800–1,000 km wide in Pangea times. Since the Neo-Tethys Ocean opened in the Middle Triassic (~240 Ma) and started closing in the Middle Jurassic (~170 Ma) we may calculate an average full spreading rate of ~1–2 cm/yr. This spreading rate, together with the recognition of the Mirdita oceanic detachment fault (e.g., Maffione et al., 2013), and the reduced thickness of the MOR-affinity ophiolites (e.g., Nicolas et al., 1999) provide strong evidence for the slow spreading nature of the Neo-Tethys. Because oceanic detachment faults are very common in slow spreading oceans (e.g., Smith et al., 2006), a well-developed detachment system may have provided the ideal conditions for subduction initiation close and parallel to the Neo-Tethyan ridge in the Middle Jurassic (Maffione, Thieulot, et al., 2015).

5.3. East Vardar Ophiolites and Their Enigmatic Plate Kinematic Context

The East Vardar Ophiolites have received much less attention from the scientific community, due to their limited exposure and highly dismembered nature. What was known previously is that they formed around the same time as the West Vardar Ophiolites and were emplaced onto the European margin (e.g., Schmid et al., 2008). Our new results from the Ibar ophiolite in central Serbia (sites AL and PR) indicating initial N-S trending dykes now demonstrate that the northern domain of the East Vardar Ophiolites formed also with similar spreading directions as the West Vardar Ophiolites (Figure 6).

The age of these rocks is not directly constrained in Serbia, but quartzdiorite intrusions pinpoint their minimum age at 168.4 ± 6.7 (Resimić-Šarić et al., 2005), which is consistent with the ages of the East Vardar Ophiolites in Macedonia and northern Greece (Božović et al., 2013; Kukoč et al., 2015; Spray et al., 1984; Zachariadis, 2007). The boninitic signature of site AL (Marroni et al., 2004) is most straightforwardly interpreted as showing that these dykes formed in the forearc of an intraoceanic subduction zone. Because the ages of the East Vardar Ophiolites are also very similar along-strike, we infer that the Ibar ophiolite of Serbia formed at a spreading center located in a forearc position above a N-S trending subduction zone. The regional direction (eastward onto the European margin) and timing (Late Jurassic-Early Cretaceous) of emplacement further suggests that this trench was different from and located east of the one associated with the West Vardar Ophiolites.

Farther south in northern Greece, the sheeted dykes from the Guevgueli ophiolite were restored to an initial NW-SE orientation, hence subparallel to the Othris ophiolite ridge in the west (Figure 6). Because the Guevgueli ophiolite has a back-arc geochemical signature (Saccani et al., 2008), we interpret the initial orientation of the sheeted dykes as reflecting the orientation of a back-arc spreading center. Because back-arc ridges are generally parallel to the associated subduction zones, we infer that the subduction zone that

governed Guevgueli back-arc spreading was NW-SE striking in northern Greece. Because the Guevgueli ophiolite appears to have formed close to a continent-derived block found in the Paikon arc (e.g., Brown & Robertson, 2004) we infer that the overriding plate of this subduction zone also contained continental crust.

Our data thus suggest that the subduction zone associated with the East Vardar Ophiolites curved southward from N-S (Serbia), to NW-SE (northern Greece), probably following the shape of the European passive margin (i.e., Moesian platform), as well as the Neo-Tethyan ridge (Figure 7). Toward the east, the trenches along the southern Pontides had a ENE-WSW orientation, both the Paleo-Tethys trench inferred to the north and the Neo-Tethys trench to the south of the Sakarya terrane (Figure 7).

As mentioned before, bringing the trench(es) associated with the East Vardar Ophiolites into the regional plate kinematic context is challenging, mainly due to the enigmatic fate of the Paleo-Tethys Ocean, whose nature and position of its suture zone is debated (e.g., Stampfli et al., 2003; Moix et al., 2008). On the one hand, several authors suggested that these ophiolites formed above a Europe-dipping subduction zone that formed along the passive margin of Eurasia, that is, after Paleo-Tethys closure (e.g., Brown & Robertson, 2004; Saccani et al., 2008). This hypothesis is based on the inferred association of the ophiolites and Europe-derived continental crust in the overriding plate of this subduction zone. This Europe-dipping subduction zone would then have been characterized by forearc intraoceanic spreading in the north (Serbia) and back-arc spreading in the south (Guevgueli). This Europe-dipping subduction zone in the scenario of Gallhofer et al. (2017) terminated shortly after, followed by formation of an Adria-dipping subduction zone in the back-arc to explain ophiolite emplacement onto the European margin (Schmid et al., 2008). No metamorphic soles have been documented from the East Vardar Ophiolites that may constrain the initiation of subduction at the associated subduction zone. Nevertheless, considering the ages of the West and East Vardar Ophilites, the scenario of Gallhofer et al. (2017) would suggest that three subduction zones formed in the Middle Jurassic, that is, one intraoceanic at the Neo-Tethyan ridge and two at the European passive margin.

Here we tentatively propose a plate tectonically simpler alternative scenario (Figure 8), which may be tested in the future against the geological record of the continental units below the East Vardar Ophiolites. Given the plate tectonic necessity (i.e., opening of the Neo-Tethys Ocean), but absence of unambiguous geological evidence for a Paleo-Tethys suture in the Balkan geology, we propose that the subduction zone above which the East Vardar Ophiolites were formed was the active subduction that at that time was already accommodating Paleo-Tethys closure. The older Paleo-Tethys subduction zone would have formed in Triassic time (or perhaps even earlier in the Permian; Stampfli & Hochard, 2009), more likely along the Greater Adria margin, rather than at the European margin as proposed by some authors (e.g., Moix et al., 2008; Şengör & Yilmaz, 1981; Stampfli & Kozur, 2006). A Eurasia-ward rollback of the Paleo-Tethyan slab (Figure 8b) would more easily explain the opening of the Neo-Tethys as a back-arc basin in the overriding plate, as well as the back-arc geochemical signature of Triassic volcanics from the Pindos Zone of Greece (Pe-Piper & Piper, 1991).

Upper plate continental fragments (Paikon and perhaps other units of the Circum-Rhodope Belt (Schmid et al., 2008)) may have detached from the Adriatic margin and drifted toward Europe following Paleo-Tethys slab rollback, and representing therefore remnants of a not previously recognized conjugate margin of the Triassic Greater Adria passive margin. This Gondwana-ward subduction of the Paleo-Tethys may have extended to the east in modern Anatolia, causing the detachment of the Sakarya block from Gondwana, its subsequent northward migration, and the opening of the Neo-Tethys at its back (Şengör & Yilmaz, 1981). Paleomagnetic data indicate that the Sakarya block has been part of Eurasia at least since the Early Jurassic (Channell et al., 1996; Meijers et al., 2010), hence constraining the minimum age of Paleo-Tethys closure in the Anatolian region. On the other hand, because there was no Adria (Africa)—Europe divergence in the Jurassic (Torsvik et al., 2012), the presence of Middle Jurassic (~170 Ma) Neo-Tethyan relics in the West Vardar Ophiolites (i.e., MOR ophiolites of Mirdita, Pindos, and Othris; Maffione, Thieulot, et al., 2015) demonstrates that rollback subduction of Paleo-Tethyan lithosphere in the Balkan area must have continued until this time to sustain seafloor spreading in the Neo-Tethys but sufficiently far away from the mid-Neo-Tethys ridge so as not to contaminate it with subduction-derived fluids (Figure 8c). When the mid–Neo-Tethyan ridge became inverted at ~175 Ma, ongoing Paleo-Tethys slab rollback to the east may have induced local extension in the upper plate of the newly formed convergent boundary, causing formation of the SSZ West Vardar Ophiolites and simultaneous exhumation of its metamorphic sole (see van Hinsbergen et al.,

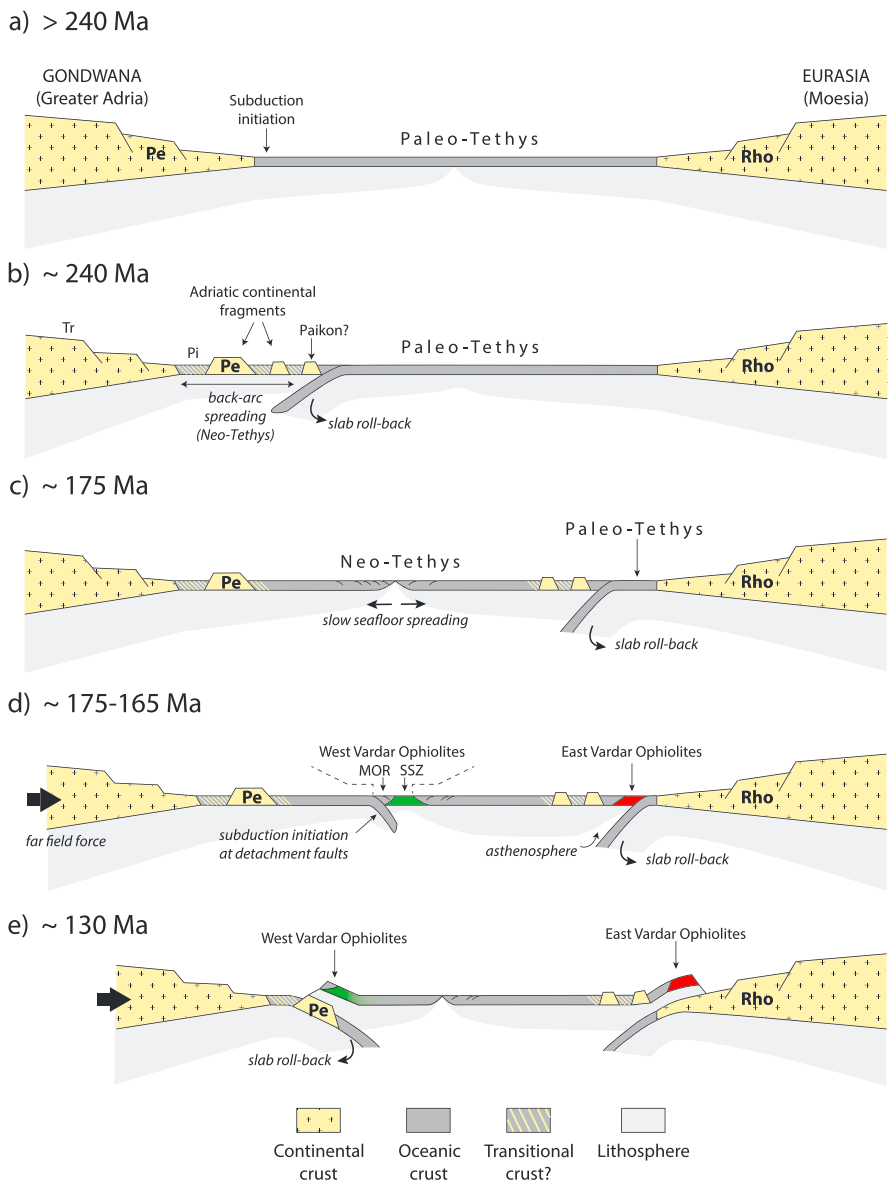

Figure 8. Speculative evolutionary cross section of the western Tethys realm (Balkan region) from the Middle Triassic to the Early Cretaceous. (a) Before the Middle Triassic (~240 Ma) a large ocean called Paleo-Tethys existed between two regions of Pangea representing the future Eurasia and Gondwana landmasses. (b) In the Middle Triassic (~240 Ma), or perhaps even earlier in the Late Permian (Stampfli & Kozur, 2006) the Neo-Tethys Ocean started to open due to subduction initiation and Europe-ward rollback of Paleo-Tethyan lithosphere. According to our new result, spreading of the Neo-Tethys in the Balkan area was E-W (N-S trending ridge). The forearc region of Gondwana underwent intense stretching during this stage, leading to the formation of several continental fragments intervened by basins (whose continental or oceanic nature is unknown), including Pelagonian (Pe) and, perhaps, Paikon and other blocks now incorporated into the Rhodope Massif. (c) In the late Early Jurassic (~175 Ma) the Neo-Tethys reached its maximum width after ~60 Ma of spreading. Due to the slow rate of spreading (1–2 cm/yr), abundant oceanic detachment faults may be present in this ocean (Maffione et al., 2013). (d) Between approximately 175 and 165 Ma, the Neo-Tethys underwent contraction, and a new subduction zone initiated near and parallel to the spreading ridge, likely along a regionally continuous detachment fault system (Maffione, Thieulot, et al., 2015). Subduction initiation was likely triggered by far-field forces associated to the coeval opening of the Alpine Tethys Ocean to the northeast. Subduction initiation at the Neo-Tethyan ridge resulted in the formation of the West Vardar Ophiolites. Because subduction started off-axis a small ribbon of MOR-affinity (Neo-Tethyan) crust was preserved in the overriding plate and subsequently incorporated into the western part of the West Vardar Ophiolite (Mirdita, Pindos, and Othris ophiolites), while suprasubduction zone (SSZ) crust was generated next to these MOR relics at a new or resumed ridge (Vourinos and Maljen ophiolites). In the east, eastward Paleo-Tethys rollback could no longer be accommodated at the Neo-Tethyan ridge due to the change in geodynamic conditions there. As a result, Paleo-Tethys rollback was accommodated instead by the formation of new forearc (Ibar) and back-arc (Guevgueli) spreading centers in the eastern margin of the overriding plate, generating the East Vardar Ophiolites. (e) In the Early Cretaceous (~130 Ma), both the West and East Vardar Ophiolites were emplaced onto the passive margins of Gondwana (Pelagonian) and Eurasia (Circum-Rhodope belt), respectively. Since the Middle Jurassic, continuous spreading of the ridge at which the West Vardar Ophiolites were formed produced melts with a progressively weaker subduction influence (i.e., fading green color). Due to the limited amount of convergence between Gondwana and Eurasia after the intraoceanic subduction initiation, a significant amount of slab rollback of Gondwanan lithosphere must have happened to enable continental emplacement of the West Vardar Ophiolites.

2015). We speculate that the changed geodynamics of the Neo-Tethyan plate following the initiation of the West Vardar subduction to the west may have affected the geodynamic equilibrium at the still active Paleo-Tethys trench in the east. This may have resulted in forearc (Serbia) and back-arc (Guevgueli) spreading in the overriding plate above the ongoing Paleo-Tethys slab rollback, leading to the formation of the East Vardar Ophiolites (Figure 8d). This scenario would imply that West Vardar subduction initiation, which may have been driven by an eastward push exerted by Middle Jurassic Central Atlantic and Alpine Tethys ocean spreading to the west (Maffione, Thieulot, et al., 2015), slightly predated full Paleo-Tethys closure in the Balkan area.

Our admittedly speculative model would require only one subduction zone (instead of three) during the Middle Jurassic in the eastern Neo-Tethys and is thus kinematically simpler. It would, however, also imply that SSZ ophiolites may also form above mature subduction zones upon sudden changes in the subduction dynamics, which would challenge, or at least add to, current ideas on their association with subduction initiation (e.g., Stern et al., 2012; van Hinsbergen et al., 2015). This hypothesis, therefore, awaits further testing. Given the ongoing debate on the subduction history of the East Vardar ophiolites, we portray in our plate kinematic configuration of the Middle Jurassic a single Adria-dipping subduction zone to the east of the East Vardar Ophiolites, close and parallel to the Eurasian margin (Figure 7).

5.4. Kinematic Connection of the West Vardar and Izmir-Ankara Jurassic Ophiolites of Northern Turkey

According to our reconstruction and the available ophiolite and metamorphic sole ages, the West Vardar and Izmir-Ankara Jurassic ophiolites formed above subduction zones that formed in the Early-Mid Jurassic (Figure 7). Crustal and metamorphic ages of the ophiolites from the Izmir-Ankara suture zone (Çelik et al., 2011, 2013; Çörtük et al., 2016; Dilek & Thy, 2006; Robertson et al., 2013; Topuz et al., 2014; Uysal et al., 2015) seem to indicate a slightly earlier subduction initiation in the eastern domain of the Neo-Tethys (late Early Jurassic; ~185–180 Ma) than in the west where it started in the Middle Jurassic (~175 Ma). Furthermore, paleomagnetic data from the Pontides indicate that subduction in the Anatolian area started once the Sakarya terrane was already part of the Eurasian margin (Channell et al., 1996; Meijers et al., 2010), hence after or perhaps during the latest stages of the Paleo-Tethys closure.

The connection between the oceans in the Balkan and Anatolian region during the Middle Jurassic has been proposed by several authors in the past (e.g., Bortolotti et al., 2017; Marroni et al., 2014; Robertson, 2002; Robertson et al., 2013) using different paleogeographic models. These paleogeographic reconstructions can now be refined by constraining the geometry of plate boundaries (in particular subduction zones) in the Neo-Tethyan realm. Based on our new results and the available geological evidence, we argue that the West Vardar subduction zone that initiated near the Neo-Tethyan ridge did not extend to the east along the same plate boundary (Figure 7). Had subduction initiated with a Europe-directed polarity along the Neo-Tethys ridge in both the Dinaric-Hellenic and Anatolian segments, Jurassic ophiolites of the Izmir-Ankara suture would have obducted onto the Greater Adriatic units of Anatolia. Cretaceous ophiolites that formed due to the earlier (~100 Ma) subduction initiation event within the Neo-Tethys north of Greater Adria in Anatolia (e.g., Maffione et al., 2017) should then have thrust onto already obducted Jurassic ophiolites, which is nowhere observed in Turkey. Instead, the Jurassic ophiolites are found north of, and structurally above the Cretaceous ophiolites of Turkey, which directly overlie Greater Adriatic units. Hence, we follow the previous inferences of, for example, Topuz et al. (2013, 2014) that the Jurassic ophiolites of the Izmir-Ankara suture formed not at the Neo-Tethyan ridge but instead in the forearc of Sakarya above a Europe-ward (i.e., N dipping) subduction zone (Figure 7). The wide range of ages of the magmatic rocks of the Izmir-Ankara mélange, spanning Jurassic and Cretaceous times (e.g., Bortolotti et al., 2017), is in fact consistent with a continuous magmatic activity at the Neo-Tethyan ridge in the Anatolian domain until at least the Middle-Upper Cretaceous.

On the other hand, the demise of these two subduction zones across western and central Neo-Tethys was not synchronous. The West Vardar subduction zone was active until at least the Early Cretaceous, when the West Vardar Ophiolites were emplaced onto Greater Adria. Subduction below the Pontides remained active throughout the Mesozoic, as shown by, for example, arc volcanism and metamorphism in the Pontide geology (e.g., Çimen et al., 2017; Okay et al., 2006, 2013). From the Middle Jurassic to earliest Cretaceous, a plate boundary must thus have existed that connected the West Vardar and Izmir-Ankara trenches. In its simplest

form, this plate boundary was a left-lateral transform fault, which we conceptually include in our paleogeographic model (Figure 7).

Finally, the Intra-Pontide suture with Middle Jurassic ophiolites, ophiolitic mélanges, and HP metamorphic rocks indicates that spreading occurred in another ocean basin in the Early-Middle Jurassic (~180–170 Ma) at the southern margin of Eurasia (Göncüoglu et al., 2012, 2014; Marroni et al., 2014; Okay et al., 2013; Şengör & Yilmaz, 1981; Ustaömer & Robertson, 1999). Various models suggesting the occurrence of multiple subduction zones at the southern margin of Eurasia have been proposed to explain the synchronous formation of the Intra-Pontide and Izmir-Ankara ophiolites, and their possible connection with the Balkan ophiolites (e.g., Bortolotti et al., 2017; Göncüoglu et al., 2014; Marroni et al., 2014; Robertson, 2002; Ustaömer & Robertson, 1999). Although beyond the scope of the current study, we consider two possible scenarios for the evolution of the Intra-Pontide suture. We speculate that the Intra-Pontide oceanic basin may have formed as a back-arc basin above the nascent northward subduction zone below the Sakarya terrane, accommodating the extension that eastward was accommodated by forming the forearc ophiolites south of Sakarya. Alternatively, the Intra-Pontide ophiolites may be equivalent to the East Vardar ophiolites and—in analogy to the scenario postulated above—may then have formed in the forearc above a southward subducting Paleo-Tethys slab during the latest stages of the Paleo-Tethys closure.

6. Conclusions

Reconstructing the initial orientation of sheeted dykes from the West and East Vardar Ophiolites of Serbia and Greece, which were previously shown to have MOR (Othris and Pindos), SSZ (Vourinos and Maljen), and BAB (Guevgueli) geochemical affinities, was used to determine the configuration of spreading ridges and trenches in the Neo-Tethys Ocean during the beginning of its closure in the Middle Jurassic. We then used our new data, together with existing geochemical, geochronological, and geological evidence from the Balkan Peninsula and northern Turkey, to reconstruct the following sequence of tectonic events:

1. The Neo-Tethyan ridge in the area of the modern Balkans prior to its inversion had an ~N-S trend, which was slightly Europe-ward concave, probably reflecting the shape of the adjacent continental margins. The opening of the Neo-Tethys was slow (i.e., 1–2 cm/yr) and directed roughly E-W;
2. Around 175 Ma, cessation of spreading at the Neo-Tethyan ridge and the initiation of a Europe-dipping subduction zone occurred. This subduction zone formed near and parallel to the N-S trending Neo-Tethyan ridge, most likely along a young oceanic detachment fault system, and resulted in the formation of the West Vardar Ophiolites along forearc ~N-S trending ridges;
3. The West Vardar Ophiolites and associated subduction zone must have terminated to the west against a plate boundary, likely a transform fault. To the west of this transform, the subduction zone continued below the southern passive margin of Europe (i.e., the Pontides of northern Turkey), where the Early-Middle Jurassic Izmir-Ankara ophiolites were formed, with the Neo-Tethyan ridge being located south of this trench;
4. Simultaneous with the initiation of the West Vardar subduction, the East Vardar Ophiolites were formed near the passive margin of Europe at a N-S to NW-SE spreading ridge parallel to the European passive margin. These ophiolites formed above a subduction zone that mimicked the shape of the ophiolitic ridges and that was located to the east of the West Vardar subduction;
5. We propose an alternative scenario in which the East Vardar Ophiolites formed by forearc and back-arc spreading above an existing Adria-dipping subduction zone that was accommodating the closure of the Paleo-Tethys Ocean since the Triassic. Upper plate spreading associated to the formation of the East Vardar Ophiolites may have then been caused by a change in the Neo-Tethyan plate dynamics after the inception of the West Vardar subduction. Our speculative model provides a kinematically simpler solution, where only one subduction zone (rather than three) formed within the Neo-Tethys in the Middle Jurassic.

Acknowledgments
M. M. and D. J. J. vH. acknowledge funding through an ERC Starting grant (to D. J. J. vH., project 306810–SINK) and an NWO VIDI grant (to D. J. J. vH., project 86411004). We thank Noortje van Rijsingen for her help in the field in Greece and for the laboratory analyses of the Greek ophiolite samples. We are thankful to Vladica Cvetković and Kristina Šarić and Liviu Matenco for providing advice on suitable field locations in Serbia and Greece. We thank Ayten Koç for her help in the field in Serbia. Fruitful discussion with Stefan Schmid greatly helped to clarify critical aspects of the complex geology of the Balkan Peninsula. We are thankful to Michele Marroni and an anonymous reviewer for constructive comments, which helped to substantially improve the original manuscript. All data presented in this paper are available in the supporting information.

References

Allerton, S., & Vine, F. J. (1987). Spreading structure of the Troodos ophiolite, Cyprus: Some paleomagnetic constraints. *Geology*, *15*(7), 593. https://doi.org/10.1130/0091-7613(1987)15<593:SSOTTO>2.0.CO;2

Anders, B., Reischmann, T., Poller, U., & Kostopoulos, D. (2005). Age and origin of granitic rocks of the eastern Vardar Zone, Greece: New constraints on the evolution of the Internal Hellenides. *Journal of the Geological Society of London*, *162*(5), 857–870. https://doi.org/10.1144/0016-764904-077

Anonymous (1972). Penrose field conference on Ophiolites. *Geotimes*, *17*, 24–25.
Barth, M. G., & Gluhak, T. M. (2009). Geochemistry and tectonic setting of mafic rocks from the Othris Ophiolite, Greece. *Contributions to Mineralogy and Petrology*, *157*(1), 23–40. https://doi.org/10.1007/s00410-008-0318-9
Barth, M. G., Mason, P. R. D., Davies, G. R., & Drury, M. R. (2008). The Othris Ophiolite, Greece: A snapshot of subduction initiation at a mid-ocean ridge. *Lithos*, *100*(1-4), 234–254. https://doi.org/10.1016/j.lithos.2007.06.018
Bazylev, B. A., Popević, A., Karamata, S., Kononkova, N. N., Simakin, S. G., Olujić, J., et al. (2009). Mantle peridotites from the Dinaridic ophiolite belt and the Vardar zone western belt, central Balkan: A petrological comparison. *Lithos*, *108*(1-4), 37–71. https://doi.org/10.1016/j.lithos.2008.09.011
Bébien, J. (1977). Mafic and ultramafic rocks associated with granites in the Vardar zone. *Nature*, *270*(5634), 232–234. https://doi.org/10.1038/270232a0
Bébien, J., Baroz, F., Capedri, S., & Venturelli, G. (1987). Magmatisme basique associé a l'ouverture d'un bassin marginal dans les Hellénides Internes au Jurassique. *Ofioliti*, *12*, 53–70.
Bébien, J., & Mercier, J. L. (1977). Le cadre structural de l9association ophiolites-migmatites-granites de Guevgueli (Macedoine, Grece); une croute de bassin interarc? *Bulletin de la Société géologique de France*, *7*(4), 927–934.
Beccaluva, L., Ohnenstetter, D., Ohnenstetter, M., & Paupy, A. (1984). Two magmatic series with island arc affinities within the vourinos ophiolite. *Contributions to Mineralogy and Petrology*, *85*(3), 253–271. https://doi.org/10.1007/BF00378104
Bernoulli, D., & Laubscher, H. (1972). The palinspastic problem of the Hellenides. *Eclogae Geologicae Helvetiae*, *65*(1), 1007–1118.
Bortolotti, V., Chiari, M., Göncüoglu, M. C., Principi, G., Saccani, E., Tekin, U. K., & Tassinari, R. (2017). The Jurassic–Early Cretaceous basalt–chert association in the ophiolites of the Ankara Mélange, east of Ankara, Turkey: Age and geochemistry. *Geological Magazine*, *155*(02), 451–478. https://doi.org/10.1017/S0016756817000401
Bortolotti, V., Chiari, M., Marroni, M., Pandolfi, L., Principi, G., & Saccani, E. (2013). Geodynamic evolution of ophiolites from Albania and Greece (Dinaric-Hellenic belt): One, two, or more oceanic basins? *International Journal of Earth Sciences*, *102*(3), 783–811. https://doi.org/10.1007/s00531-012-0835-7
Bortolotti, V., Chiari, M., Marcucci, M., Photiades, A., Principi, G., & Saccani, E. (2008). New geochemical and age data on the ophiolites from the Othrys area (Greece): Implication for the Triassic evolution of the Vardar ocean. *Ofioliti*, *33*(2), 135–151.
Bortolotti, V., Marroni, M., Pandolfi, L., & Principi, G. (2005). Mesozoic to tertiary tectonic history of the Mirdita ophiolites, northern Albania. *Island Arc*, *14*(4), 471–493. https://doi.org/10.1111/j.1440-1738.2005.00479.x
Bortolotti, V., Marroni, M., Pandolfi, L., Principi, G., & Saccani, E. (2002). Interaction between Mid-Ocean Ridge and Subduction Magmatism in Albanian Ophiolites. *Journal of Geology*, *110*(5), 561–576. https://doi.org/10.1086/341758
Bortolotti, V., & Principi, G. (2005). Tethyan ophiolites and Pangea break-up. *Island Arc*, *14*(4), 442–470. https://doi.org/10.1111/j.1440-1738.2005.00478.x
Božović, M., Prelević, D., Romer, R. L., Barth, M., Van Den Bogaard, P., & Boev, B. (2013). The demir kapija ophiolite, Macedonia (FYROM): A Snapshot of subduction initiation within a back-arc. *Journal of Petrology*, *54*(7), 1399–1425. https://doi.org/10.1093/petrology/egt016
Brown, S. A. M., & Robertson, A. H. F. (2004). Evidence for Neotethys rooted within the Vardar suture zone from the Voras Massif, northernmost Greece. *Tectonophysics*, *381*(1-4), 143–173. https://doi.org/10.1016/j.tecto.2002.06.001
Brun, J.-P., & Sokoutis, D. (2007). Kinematics of the southern Rhodope core complex (Northern Greece). *International Journal of Earth Sciences*, *96*(6), 1079–1099. https://doi.org/10.1007/s00531-007-0174-2
Carosi, R., Cortesogno, L., Gaggero, L., & Marroni, M. (1996). Geological and petrological features of the metamorphic sole from the Mirdita nappe, northern Albania. *Ofioliti*, *21*(1).
Casey, J. F., & Dewey, J. F. F. (1984). Initiation of subduction zones along transform and accreting plate boundaries, triple-junction evolution, and forearc spreading centres—Implications for ophiolitic geology and obduction. *Geological Society of London, Special Publication*, *13*(1), 269–290. https://doi.org/10.1144/GSL.SP.1984.013.01.22
Çelik, Ö. F., Chiaradia, M., Marzoli, A., Billor, Z., & Marschik, R. (2013). The Eldivan ophiolite and volcanic rocks in the İzmir–Ankara–Erzincan suture zone, Northern Turkey: Geochronology, whole-rock geochemical and Nd–Sr–Pb isotope characteristics. *Lithos*, *172*, 31–46.
Çelik, Ö. F., Delaloye, M., & Feraud, G. (2006). Precise ^{40}Ar– ^{39}Ar ages from the metamorphic sole rocks of the Tauride Belt Ophiolites, southern Turkey: Implications for the rapid cooling history. *Geological Magazine*, *143*(02), 213. https://doi.org/10.1017/S0016756805001524
Çelik, Ö. F., Marzoli, A., Marschik, R., Chiaradia, M., Neubauer, F., & Öz, İ. (2011). Early–Middle Jurassic intra-oceanic subduction in the İzmir-Ankara-Erzincan Ocean, Northern Turkey. *Tectonophysics*, *509*(1-2), 120–134. https://doi.org/10.1016/j.tecto.2011.06.007
Çelik, T. F., Chiaradia, M., Marzoli, A., Özkan, M., Billor, Z., & Topuz, G. (2016). Jurassic metabasic rocks in the Kizilirmak accretionary complex (Kargi region, Central Pontides, Northern Turkey). *Tectonophysics*, *672-673*, 34–49. https://doi.org/10.1016/j.tecto.2016.01.043
Channell, J. E. T., Tüysüz, O., Bektas, O., & Sengör, A. M. C. (1996). Jurassic-Cretaceous paleomagnetism and paleogeography of the Pontides (Turkey). *Tectonics*, *15*(1), 201–212. https://doi.org/10.1029/95TC02290
Chiari, M., Bortolotti, V., Marcucci, M., Photiades, A., & Principi, G. (2003). The middle Jurassic siliceous sedimentary cover at the top of the vourinos ophiolite (Greece). *Ofioliti*, *28*(2), 95–103.
Chiari, M., Djerić, N., Garfagnoli, F., Hrvatović, H., Krstić, M., Levi, N., et al. (2011). The geology of the Zlatibor-Maljen area (western Serbia): A geotraverse across the ophiolites of the Dinaric-Hellenic collisional belt. *Ofioliti*, *36*(2), 139–166.
Chiari, M., Marcucci, M., & Prela, M. (1994). Mirdita ophiolites project: 2 radiolarian assemblages in the cherts at Fushe Arrez and Shebaj (Mirdita area, Albania). *Ofioliti*, *19*(2).
Christofides, G., D'amico, C., Del Moro, A., Eleftheriadis, G., & Kyriakopoulos, C. (1990). Rb/Sr geochronology and geochemical characters of the Sithonia plutonic complex (Greece). *European Journal of Mineralogy*, *2*(1), 79–88. https://doi.org/10.1127/ejm/2/1/0079
Çimen, O., Cemal Göncüoğlu, M., Simonetti, A., & Sayıt, K. (2017). Whole rock geochemistry, Zircon U-Pb and Hf isotope systematics of the Çangaldağ Pluton: Evidences for Middle Jurassic Continental Arc Magmatism in the Central Pontides, Turkey. *Lithos*, *290-291*, 136–155. https://doi.org/10.1016/j.lithos.2017.06.020
Çörtük, R. M., Çelik, Ö. F., Özkan, M., Sherlock, S. C., Marzoli, A., Altıntaş, İ. E., & Topuz, G. (2016). Origin and geodynamic environments of the metamorphic sole rocks from the İzmir–Ankara–Erzincan suture zone (Tokat, northern Turkey). *International Geology Review*, *58*(15), 1839–1855. https://doi.org/10.1080/00206814.2016.1181991
Danelian, T., Robertson, A. H. F., & Dimitriadis, S. (1996). Age and significance of radiolarian sediments within basic extrusives of the marginal basin Guevgueli Ophiolite (northern Greece). *Geological Magazine*, *133*(02), 127–136. https://doi.org/10.1017/S0016756800008645
Day, R., Fuller, M., & Schmidt, V. A. (1977). Hysteresis properties of titanomagnetites: Grain-size and compositional dependence. *Physics of the Earth and Planetary Interiors*, *13*(4), 260–267. https://doi.org/10.1016/0031-9201(77)90108-X
Deenen, M. H. L., Langereis, C. G., van Hinsbergen, D. J. J., & Biggin, A. J. (2011). Geomagnetic secular variation and the statistics of palaeomagnetic directions. *Geophysical Journal International*, *186*(2), 509–520. https://doi.org/10.1111/j.1365-246X.2011.05050.x

Dewey, J. F., & Casey, J. F. (2013). The sole of an ophiolite: The Ordovician Bay of Islands Complex, Newfoundland. *Journal of the Geological Society, London*, *170*(5), 715–722. https://doi.org/10.1144/jgs2013-017

Dijkstra, A. H., Drury, M. R., & Vissers, R. L. M. (2001). Structural petrology of plagioclase peridotites in the West Othris Mountains (Greece): Melt impregnation in mantle lithosphere. *Journal of Petrology*, *42*(1), 5–24. https://doi.org/10.1093/petrology/42.1.5

Dilek, Y., & Furnes, H. (2011). Ophiolite genesis and global tectonics: Geochemical and tectonic fingerprinting of ancient oceanic lithosphere. *Bulletin Geological Society of America*, *123*(3-4), 387–411. https://doi.org/10.1130/B30446.1

Dilek, Y., Furnes, H., & Shallo, M. (2008). Geochemistry of the Jurassic Mirdita Ophiolite (Albania) and the MORB to SSZ evolution of a marginal basin oceanic crust. *Lithos*, *100*(1-4), 174–209. https://doi.org/10.1016/j.lithos.2007.06.026

Dilek, Y., & Thy, P. (2006). Age and petrogenesis of plagiogranite intrusions in the Ankara melange, central Turkey. *Island Arc*, *15*(1), 44–57. https://doi.org/10.1111/j.1440-1738.2006.00522.x

Dimitrijević, M. D. (1997). *Geology of Yugoslavia* (p. 187). Belgrade: Geological Institute GEMINI Special Publication.

Dimo-Lahitte, A., Monié, P., & Vergély, P. (2001). Metamorphic soles from the Albanian ophiolites: Petrology, $^{40}Ar/^{39}Ar$ geochronology, and geodynamic evolution. *Tectonics*, *20*(1), 78–96. https://doi.org/10.1029/2000TC900024

Dokuz, A., Aydınçakır, E., Kandemir, R., Karslı, O., Siebel, W., Derman, A. S., & Turan, M. (2017). Late Jurassic magmatism and stratigraphy in the eastern Sakarya zone, Turkey: Evidence for the slab breakoff of Paleotethyan oceanic lithosphere. *The Journal of Geology*, *125*(1), 1–31. https://doi.org/10.1086/689552

Dunlop, D. J. (2002). Theory and application of the Day plot (M-rs/M-s versus H-cr/H-c) 1. Theoretical curves and tests using titanomagnetite data. *Journal of Geophysical Research*, *107*(B3), 2056. https://doi.org/10.1029/2001JB000486

Dunlop, D. J., & Özdemir, Ö. (1997). *Rock magnetism: Fundamentals and frontiers* (573 pp.). New York: Cambridge University Press. https://doi.org/10.1017/CBO9780511612794

Ferriére, J. (1982). Paléogéographie et tectonique superpose oes dans les Hellenides internes: Les massifs de l'Othrys et du Pélion (Gréce septentrionale). *Société de la Géologie du Nord*, *8*, 1–970.

Fisher, R. A. (1953). Dispersion on a sphere. *Proceedings of the Royal Society London*, *217*(1130), 295–305. https://doi.org/10.1098/rspa.1953.0064

Franke, W., Cocks, L. R. M., & Torsvik, T. H. (2017). The Palaeozoic Variscan oceans revisited. *Gondwana Research*, *48*, 257–284. https://doi.org/10.1016/j.gr.2017.03.005

Gaggero, L., Marroni, M., Pandolfi, L., & Buzzi, L. (2009). Modeling the oceanic lithosphere obduction: Constraints from the metamorphic sole of Mirdita ophiolites (northern Albania). *Ofioliti*, *34*(1), 17–42.

Gaina, C., Torsvik, T. H., van Hinsbergen, D. J. J., Medvedev, S., Werner, S. C., & Labails, C. (2013). The African Plate: A history of oceanic crust accretion and subduction since the Jurassic. *Tectonophysics*, *604*, 4–25. https://doi.org/10.1016/j.tecto.2013.05.037

Gallhofer, D., Von Quadt, A., Schmid, S. M., Guillong, M., Peytcheva, I., & Seghedi, I. (2017). Magmatic and tectonic history of Jurassic ophiolites and associated granitoids from the South Apuseni Mountains (Romania). *Swiss Journal of Geosciences*, *110*(2), 699–719. https://doi.org/10.1007/s00015-016-0231-6

Godfriaux, I., & Ricou, L.-E. (1991). The Paikon, a tectonic window within the Internal Hellenides, Macedonia, Greece | Le Paikon, une fenetre tectonique dans les Hellenides Internes (Macedoine, Grece). *Comptes Rendus - Academie des Sciences Series II*, *313*(12).

Göncüoglu, M. C., Marroni, M., Pandolfi, L., Ellero, A., Ottria, G., Catanzariti, R., et al. (2014). The Arkot Dağ Mélange in Araç area, central Turkey: Evidence of its origin within the geodynamic evolution of the Intra-Pontide suture zone. *Journal of Asian Earth Sciences*, *85*, 117–139. https://doi.org/10.1016/j.jseaes.2014.01.013

Göncüoglu, M. C., Marroni, M., Sayit, K., Tekin, U. K., Ottria, G., Pandolfi, L., & Ellero, A. (2012). The Ayli Dağ ophiolite sequence (central-northern Turkey): A fragment of middle Jurassic oceanic lithosphere within the Intra-Pontide suture zone. *Ofioliti*, *37*(2), 77–92.

Granot, R. (2016). Palaeozoic-aged oceanic crust preserved beneath the eastern Mediterranean. *Nature Geoscience*, *9*(9), 701–705. https://doi.org/10.1038/ngeo2784

Guilmette, C., Hébert, R., Wang, C., & Villeneuve, M. (2009). Geochemistry and geochronology of the metamorphic sole underlying the Xigaze Ophiolite, Yarlung Zangbo Suture Zone, South Tibet. *Lithos*, *112*(1-2), 149–162. https://doi.org/10.1016/j.lithos.2009.05.027

Gürer, D., van Hinsbergen, D. J. J., Matenco, L., Corfu, F., & Cascella, A. (2016). Kinematics of a former plate revealed by forearc deformation: The Ulukisla basin and the tale of the Anadolu Plate. *Tectonics*, *35*, 2385–2416. https://doi.org/10.1002/2016TC004206

Hoeck, V., Ionescu, C., Balintoni, I., & Koller, F. (2009). The Eastern Carpathians "ophiolites" (Romania): Remnants of a Triassic ocean. *Lithos*, *108*(1-4), 151–171. https://doi.org/10.1016/j.lithos.2008.08.001

Hoeck, V., Koller, F., Meisel, T., Onuzi, K., & Kneringer, E. (2002). The Jurassic South Albanian ophiolites: MOR- vs. SSZ-type ophiolites. *Lithos*, *65*(1-2), 143–164. https://doi.org/10.1016/S0024-4937(02)00163-9

Huang, W., van Hinsbergen, D. J. J., Maffione, M., Orme, D. A., Dupont-Nivet, G., Guilmette, C., et al. (2015). Lower Cretaceous Xigaze ophiolites formed in the Gangdese forearc: Evidence from paleomagnetism, sediment provenance, and stratigraphy. *Earth and Planetary Science Letters*, *415*, 142–153. https://doi.org/10.1016/j.epsl.2015.01.032

Hurst, S. D., Verosub, K. L., & Moores, E. M. (1992). Paleomagnetic constraints on the formation of the Solea graben, Troodos ophiolite, Cyprus. *Tectonophysics*, *208*(4), 431–445. https://doi.org/10.1016/0040-1951(92)90439-D

Inwood, J., Morris, A., Anderson, M. W., & Robertson, A. H. F. F. (2009). Neotethyan intraoceanic microplate rotation and variations in spreading axis orientation: Palaeomagnetic evidence from the Hatay ophiolite (southern Turkey). *Earth and Planetary Science Letters*, *280*(1-4), 105–117. https://doi.org/10.1016/j.epsl.2009.01.021

Johnson, C. L., Constable, C. G., Tauxe, L., Barendregt, R., Brown, L. L., Coe, R. S., et al. (2008). Recent investigations of the 0–5 Ma geomagnetic field recorded by lava flows. *Geochemistry, Geophysics, Geosystems*, *9*, Q04032. https://doi.org/10.1029/2007GC001696

Jones, G., & Robertson, A. H. (1991). Tectono-stratigraphy and evolution of the Mesozoic Pindos ophiolite and related units, northwestern Greece. *Journal of the Geological Society of London*, *148*(2), 267–288. https://doi.org/10.1144/gsjgs.148.2.0267

Kapsiotis, A. N. (2014). Compositional signatures of SSZ-type peridotites from the northern Vourinos ultra-depleted upper mantle suite, NW Greece. *Chemie der Erde-Geochemistry*, *74*(4), 783–801. https://doi.org/10.1016/j.chemer.2014.05.004

Karamata, S. (2006). The geological development of the Balkan Peninsula related to the approach, collision and compression of Gondwanan and Eurasian units. *Geological Society, London, Special Publications*, *260*(1), 155–178. https://doi.org/10.1144/GSL.SP.2006.260.01.07

Kirschvink, J. L. (1980). The least-squares line and plane and the analysis of palaeomagnetic data. *Geophysical Journal International*, *62*(3), 699–718. https://doi.org/10.1111/j.1365-246X.1980.tb02601.x

Kondopoulou, D., & Westphal, M. (1986). Paleomagnetism of the tertiary intrusives from Chalkidiki (northern Greece). *Journal of Geophysics*, *59*, 62–66.

Koymans, M. R., Langereis, C. G., Pastor-Galán, D., & van Hinsbergen, D. J. J. (2016). Paleomagnetism.org: An online multi-platform open source environment for paleomagnetic data analysis. *Computational Geosciences*, *93*, 127–137. https://doi.org/10.1016/j.cageo.2016.05.007

Kukoč, D., Goričan, Š., Košir, A., Belak, M., Halamić, J., & Hrvatović, H. (2015). Middle Jurassic age of basalts and the post-obduction sedimentary sequence in the Guevgueli Ophiolite Complex (Republic of Macedonia). *International Journal of Earth Sciences*, *104*(2), 435–447. https://doi.org/10.1007/s00531-014-1086-6

Labails, C., Olivet, J.-L., Aslanian, D., & Roest, W. R. (2010). An alternative early opening scenario for the Central Atlantic Ocean. *Earth and Planetary Science Letters*, *297*(3-4), 355–368. https://doi.org/10.1016/j.epsl.2010.06.024

Liati, A., Gebauer, D., & Fanning, C. M. M. (2004). The age of ophiolitic rocks of the Hellenides (Vourinos, Pindos, Crete): First U-Pb ion microprobe (SHRIMP) zircon ages. *Chemical Geology*, *207*(3-4), 171–188. https://doi.org/10.1016/j.chemgeo.2004.02.010

Maffione, M., Morris, A., & Anderson, M. W. (2013). Recognizing detachment-mode seafloor spreading in the deep geological past. *Scientific Reports*, *3*(1), 2336. https://doi.org/10.1038/srep02336

Maffione, M., Thieulot, C., van Hinsbergen, D. J. J., Morris, A., Plümper, O., & Spakman, W. (2015). Dynamics of intraoceanic subduction initiation: 1. Oceanic detachment fault inversion and the formation of supra-subduction zone ophiolites. *Geochemistry, Geophysics, Geosystems*, *16*, 1771–1785. https://doi.org/10.1002/2015GC005745

Maffione, M., van Hinsbergen, D. J. J., de Gelder, G. I. N. O., van der Goes, F. C., & Morris, A. (2017). Kinematics of Late Cretaceous subduction initiation in the Neo-Tethys Ocean reconstructed from ophiolites of Turkey, Cyprus, and Syria. *Journal of Geophysical Research: Solid Earth*, *122*, 3953–3976. https://doi.org/10.1002/2016JB013821

Maffione, M., van Hinsbergen, D. J. J., Koornneef, L. M. T., Guilmette, C., Hodges, K., Borneman, N., et al. (2015). Forearc hyperextension dismembered the south Tibetan ophiolites. *Geology*, *43*(6), 475–478. https://doi.org/10.1130/G36472.1

Marcucci, M., Kodra, A., Pirdeni, A., & Gjata, T. (1994). Radiolarian assemblages in the Triassic and Jurassic cherts of Albania. *Ofioliti*, *19*(1).

Marcucci, M., & Prela, M. (1996). The Lumi i Zi (Puke) section of the Kalur Cherts: Radiolarian assemblages and comparison with other sections in northern Albania. *Ofioliti*, *21*(1), 71–76.

Marroni, M., Frassi, C., Göncüoğlu, M. C., Di Vincenzo, G., Pandolfi, L., Rebay, G., et al. (2014). Late Jurassic amphibolite-facies metamorphism in the Intra-Pontide Suture Zone (Turkey): An eastward extension of the Vardar Ocean from the Balkans into Anatolia? *Journal of the Geological Society*, *171*(5), 605–608. https://doi.org/10.1144/jgs2013-104

Marroni, M., Pandolfi, L., Saccani, E., & Zelic, M. (2004). Boninites from the Kopaonik area (Southern Serbia): New evidences for suprasubduction ophiolites in the Vardar zone. *Ofioliti*, *29*(2), 251–254.

Márton, E., Ćosović, V., Bucković, D., & Moro, A. (2010). The tectonic development of the Northern Adriatic region constrained by Jurassic and Cretaceous paleomagnetic results. *Tectonophysics*, *490*(1-2), 93–102. https://doi.org/10.1016/j.tecto.2010.04.032

Meijers, M. J. M., Langereis, C. G., van Hinsbergen, D. J. J., Kaymakcı, N., Stephenson, R. A., & Altıner, D. (2010). Jurassic–Cretaceous low paleolatitudes from the circum-Black Sea region (Crimea and Pontides) due to True Polar Wander. *Earth and Planetary Science Letters*, *296*(3-4), 210–226. https://doi.org/10.1016/j.epsl.2010.04.052

Moix, P., Beccaletto, L., Kozur, H. W., Hochard, C., Rosselet, F., & Stampfli, G. M. (2008). A new classification of the Turkish terranes and sutures and its implication for the paleotectonic history of the region. *Tectonophysics*, *451*(1-4), 7–39. https://doi.org/10.1016/j.tecto.2007.11.044

Montigny, R., Bougault, H., Bottinga, Y., & Allegre, C. J. (1973). Trace element geochemistry and genesis of the Pindos ophiolite suite. *Geochimica et Cosmochimica Acta*, *37*(9), 2135–2147. https://doi.org/10.1016/0016-7037(73)90012-4

Moores, E. M. (1969). *Petrology and structure of the vourinos ophiolitic complex of Northern Greece* (Vol. 118). America: Geological Society. https://doi.org/10.1130/SPE118-p3

Morris, A. (1995). Rotational deformation during Palaeogene thrusting and basin closure in eastern central Greece: Palaeomagnetic evidence from Mesozoic carbonates. *Geophysical Journal International*, *121*(3), 827–847. https://doi.org/10.1111/j.1365-246X.1995.tb06442.x

Morris, A., & Anderson, M. W. (2002). Palaeomagnetic results from the Baër-Bassit ophiolite of northern Syria and their implication for fold tests in sheeted dyke terrains. *Physics and Chemistry of the Earth*, *27*(25-31), 1215–1222. https://doi.org/10.1016/S1474-7065(02)00123-7

Morris, A., Anderson, M. W., & Robertson, A. H. F. F. (1998). Multiple tectonic rotations and transform tectonism in an intraoceanic suture zone, SW Cyprus. *Tectonophysics*, *299*(1-3), 229–253. https://doi.org/10.1016/S0040-1951(98)00207-8

Morris, A., Anderson, M. W., Robertson, A. H. F. F., & Al-Riyami, K. (2002). Extreme tectonic rotations within an eastern Mediterranean ophiolite (Baäer-Bassit, Syria). *Earth and Planetary Science Letters*, *202*(2), 247–261. https://doi.org/10.1016/S0012-821X(02)00782-3

Morris, A., Creer, K. M. M., & Robertson, A. H. F. H. F. (1990). Palaeomagnetic evidence for clockwise rotations related to dextral shear along the Southern Troodos Transform Fault, Cyprus. *Earth and Planetary Science Letters*, *99*(3), 250–262. https://doi.org/10.1016/0012-821X(90)90114-D

Morris, A., & Maffione, M. (2016). Is the Troodos ophiolite (Cyprus) a complete, transform fault-bounded Neotethyan ridge segment? *Geology*, *44*(3), 199–202. https://doi.org/10.1130/G37529.1

Nicolas, A., Boudier, F., & Meshi, A. (1999). Slow spreading accretion and mantle denudation in the Mirdita ophiolite (Albania). *Journal of Geophysical Research*, *104*(B7), 15,155–15,167. https://doi.org/10.1029/1999JB900126

Okay, A. I., Sunal, G., Sherlock, S., Altıner, D., Tüysüz, O., Kylander-Clark, A. R. C., & Aygül, M. (2013). Early Cretaceous sedimentation and orogeny on the active margin of Eurasia: Southern Central Pontides, Turkey. *Tectonics*, *32*, 1247–1271. https://doi.org/10.1002/tect.20077

Okay, A. I., Tüysüz, O., Satir, M., Özkan-Altiner, S., Altiner, D., Sherlock, S., & Eren, R. H. (2006). Cretaceous and Triassic subduction-accretion, high-pressure-low-temperature metamorphism, and continental growth in the Central Pontides, Turkey. *Geological Society of America Bulletin*, *118*(9-10), 1247–1269. https://doi.org/10.1130/B25938.1

Pamić, J., Gušić, I., & Jelaska, V. (1998). Geodynamic evolution of the central Dinarides. *Tectonophysics*, *297*(1-4), 251–268. https://doi.org/10.1016/S0040-1951(98)00171-1

Pamić, J., Tomljenović, B., & Balen, D. (2002). Geodynamic and petrogenetic evolution of Alpine ophiolites from the central and NW Dinarides: An overview. *Lithos*, *65*(1-2), 113–142. https://doi.org/10.1016/S0024-4937(02)00162-7

Parlak, O. (2016). The tauride ophiolites of Anatolia (Turkey): A review. *Journal of Earth Science*, *27*(6), 901–934. https://doi.org/10.1007/s12583-016-0679-3

Parlak, O., Çolakoğlu, A., Dönmez, C., Sayak, H., Yildirim, N., Türkel, A., & Odabaşi, İ. (2013). Geochemistry and tectonic significance of ophiolites along the İzmir–Ankara–Erzincan Suture Zone in northeastern Anatolia. *Geological Society, London, Special Publications*, *372*(1), 75–105. https://doi.org/10.1144/SP372.7

Pearce, J. A., Lippard, S. J., & Roberts, S. (1984). Characteristics and tectonic significance of supra-subduction zone ophiolites. *Geological Society of London, Special Publication*, *16*(1), 77–94. https://doi.org/10.1144/GSL.SP.1984.016.01.06

Pe-Piper, G., & Piper, D. J. W. (1991). Early Mesozoic oceanic subduction-related volcanic rocks. *Tectonophysics*, *192*(3-4), 273–292. https://doi.org/10.1016/0040-1951(91)90104-Z

Photiades, A., Saccani, E., & Tassinari, R. (2003). Petrogenesis and tectonic setting of volcanic rocks from the subpelagonian ophiolitic mélange in the Agoriani area (Othrys, Greece). *Ofioliti*, *28*(2), 121–135.

Prela, M., Chiari, M., & Marcucci, M. (2000). Jurassic radiolarian biostratigraphy of the sedimentary cover of ophiolites in the Mirdita area, Albania: New data. *Ofioliti*, *25*(1), 55–62.

Rassios, A. (1981). Geology and evolution of the vourinos complex, Northern Greece. PhD. thesis. University of California (Davis), 499 pp.

Rassios, A. E., & Dilek, Y. (2009). Rotational deformation in the Jurassic Mesohellenic ophiolites, Greece, and its tectonic significance. *Lithos*, *108*(1-4), 207–223. https://doi.org/10.1016/j.lithos.2008.09.005

Reagan, M. K., Ishizuka, O., Stern, R. J., Kelley, K. A., Ohara, Y., Blichert-Toft, J., et al. (2010). Fore-arc basalts and subduction initiation in the Izu-Bonin-Mariana system. *Geochemistry, Geophysics, Geosystems*, *11*, Q03X12. https://doi.org/10.1029/2009GC002871

Resimić-Šarić, K., Cvetković, V., & Balogh, K. (2005). Radiometric K/Ar data as an evidence of the geodynamic evolution of the Ždraljica ophiolitic complex (central Serbia). *Annales Géologiques de la Péninsule Balkanique*, *66*, 73–79.

Resimić-Šarić, K., Cvetković, V., Balogh, K., & Koroneos, A. (2006). Main characteristics of ophiolitic complexes within the eastern branch of the Vardar Zone Composite Terrane in Serbia. In International Symposium on the Mesozoic ophiolite belts of the northern part of the Balkan Peninsula, Belgrade (Serbia) and Banja Luka (Bosnia and Herzegovina), p. 112–115.

Ricou, L.-E., & Godfriaux, I. (1991). A cross-section through allochthonous ophiolites and gneiss between the Pelagonian massif and the Paikon window, northern Greece | Une coupe a travers les ophiolites et gneiss allochtones entre le massif Pelagonien et la fenetre du Paikon (Grece du Nord). *Comptes Rendus - Academie des Sciences Series II*, *313*(13).

Ricou, L.-E., & Godfriaux, I. (1995). Review on the Paikon multiple window and the structure of the Vardar in Greece French with abridged English | Mise au point sur la fenetre multiple du Paikon et la structure du Vardar en Grece. *Comptes Rendus - Academie des Sciences Ser. II Sci. la Terre des Planetes*, *321*(7).

Robertson, A., Parlak, O., Ustaömer, T., Taslı, K., Dumitrica, P., & Karaoğlan, F. (2013). Subduction, ophiolite genesis and collision history of Tethys adjacent to the Eurasian continental margin: New evidence from the Eastern Pontides, Turkey. *Geodinamica Acta*, *26*(3-4), 230–293. https://doi.org/10.1080/09853111.2013.877240

Robertson, A. H. F. (2002). Overview of the genesis and emplacement of Mesozoic ophiolites in the Eastern Mediterranean Tethyan region. *Lithos*, *65*(1-2), 1–67. https://doi.org/10.1016/S0024-4937(02)00160-3

Robertson, A. H. F. (2012). Late Palaeozoic–Cenozoic tectonic development of Greece and Albania in the context of alternative reconstructions of Tethys in the Eastern Mediterranean region. *International Geology Review*, *54*(4), 373–454. https://doi.org/10.1080/00206814.2010.543791

Robertson, A. H. F., Dixon, J. E., Brown, S., Collins, A., Morris, A., Pickett, E., et al. (1996). Alternative tectonic models for the Late Palaeozoic-Early Tertiary development of Tethys in the Eastern Mediterranean region. *Geological Society, London, Special Publications*, *105*(1), 239–263. https://doi.org/10.1144/GSL.SP.1996.105.01.22

Robertson, A. H. F., & Karamata, S. (1994). The role of subduction-accretion processes in the tectonic evolution of the MesozoicTethys in Serbia. *Tectonophysics*, *234*(1-2), 73–94. https://doi.org/10.1016/0040-1951(94)90205-4

Roddick, J. C., Cameron, W. E., & Smith, A. G. (1979). Permo-Triassic and Jurassic ^{40}Ar-^{39}Ar ages from Greek ophiolites and associated rocks. *Nature*, *279*(5716), 788–790. https://doi.org/10.1038/279788a0

Saccani, E., Bortolotti, V., Marroni, M., Pandolfi, L., Photiades, A., & Principi, G. (2008). The Jurassic association of backarc basin ophiolites and calc-alkaline volcanics in the Guevgueli complex (northern Greece): Implication for the evolution of the Vardar zone. *Ofioliti*, *33*(2), 209–227.

Saccani, E., & Photiades, A. (2004). Mid-ocean ridge and supra-subduction affinities in the Pindos ophiolites (Greece): Implications for magma genesis in a forearc setting. *Lithos*, *73*(3-4), 229–253. https://doi.org/10.1016/j.lithos.2003.12.002

Šarić, K., Cvetković, V., Romer, R. L., Christofides, G., & Koroneos, A. (2009). Granitoids associated with East Vardar ophiolites (Serbia, F.Y.R. of Macedonia and northern Greece): Origin, evolution and geodynamic significance inferred from major and trace element data and Sr-Nd-Pb isotopes. *Lithos*, *108*(1-4), 131–150. https://doi.org/10.1016/j.lithos.2008.06.001

Scherreiks, R., Meléndez, G., Boudagher-Fadel, M., Fermeli, G., & Bosence, D. (2014). Stratigraphy and tectonics of a time-transgressive ophiolite obduction onto the eastern margin of the Pelagonian platform from Late Bathonian until Valanginian time, exemplified in northern Evvoia, Greece. *International Journal of Earth Sciences*, *103*(8), 2191–2216. https://doi.org/10.1007/s00531-014-1036-3

Schmid, S. M., Bernoulli, D., Fügenschuh, B., Matenco, L., Schefer, S., Schuster, R., et al. (2008). The Alpine-Carpathian-Dinaridic orogenic system: Correlation and evolution of tectonic units. *Swiss Journal of Geosciences*, *101*(1), 139–183. https://doi.org/10.1007/s00015-008-1247-3

Şengör, A. M. C., & Yilmaz, Y. (1981). Tethyan evolution of Turkey: A plate tectonic approach. *Tectonophysics*, *75*(3-4), 181–241. https://doi.org/10.1016/0040-1951(81)90275-4

Shervais, J. W. (1982). TiV plots and the petrogenesis of modern and ophiolitic lavas. *Earth and Planetary Science Letters*, *59*(1), 101–118. https://doi.org/10.1016/0012-821X(82)90120-0

Smith, A. G., & Spray, J. G. (1984). A half-ridge transform model for the Hellenic-Dinaric ophiolites. *Geological Evolution of the Eastern Mediterranean*, *17*(1), 629–644. https://doi.org/10.1144/GSL.SP.1984.017.01.49

Smith, D. K., Cann, J. R., & Escartin, J. (2006). Widespread active detachment faulting and core complex formation near 138 N on the Mid-Atlantic Ridge. *Nature*, *442*(7101), 440–443. https://doi.org/10.1038/nature04950

Soldatos, T., Koroneos, A., & Christofides, G. (1993). Origin and evolution of the Fanos granite (Macedonia, northern Greece): Trace and REE modelling constraints. *Special Volume in Honour of Professor AG Panagos. National Technical University of Athens Scientific Publications, Athens, Greece, B*, 789–812.

Sostarić, B. S., Palinkaš, A. L., Neubauer, F., Cvetković, V., Bernroider, M., & Genser, J. (2014). The origin and age of the metamorphic sole from the Rogozna Mts., Western Vardar Belt: New evidence for the one-ocean model for the Balkan ophiolites. *Lithos*, *192-195*, 39–55. https://doi.org/10.1016/j.lithos.2014.01.011

Speranza, F., Minelli, L., Pignatelli, A., & Chiappini, M. (2012). The Ionian Sea: The oldest in situ ocean fragment of the world? *Journal of Geophysical Research*, *117*, B12101. https://doi.org/10.1029/2012JB009475

Spray, J. G., Bébien, J., Rex, D. C., & Roddick, J. C. (1984). Age constraints on the igneous and metamorphic evolution of the Hellenic-Dinaric ophiolites. *Geological Society, London, Special Publications*, *17*(1), 619–627. https://doi.org/10.1144/GSL.SP.1984.017.01.48

Spray, J. G., & Roddick, J. C. (1980). Petrology and ^{40}Ar/^{39}Ar geochronology of some hellenic sub-ophiolite metamorphic rocks. *Contributions to Mineralogy and Petrology*, *72*(1), 43–55. https://doi.org/10.1007/BF00375567

Stampfli, G., Marcoux, J., & Baud, A. (1991). Tethyan margins in space and time. *Palaeogeography Palaeoclimatology Palaeoecology*, *87*(1-4), 373–409. https://doi.org/10.1016/0031-0182(91)90142-E

Stampfli, G. M., & Hochard, C. (2009). Plate tectonics of the Alpine realm (G. M. Stampfli & C. Hochard, Eds.). *Geological Society, London, Special Publications*, *327*(1), 89–111. https://doi.org/10.1144/SP327.6

Stampfli, G. M., & Kozur, H. W. (2006). Europe from the Variscan to the Alpine cycles. *Memoirs. Geological Society of London*, *32*(1), 57–82. https://doi.org/10.1144/GSL.MEM.2006.032.01.04

Stampfli, G. M., Vavassis, I., De Bono, A., Rosselet, F., Matti, B., & Bellini, M. (2003). Remnants of the Paleotethys oceanic suture-zone in the western Tethyan area. In *Stratigraphic and structural evolution on the Late Carboniferous to Triassic continental and marine successions in Tuscany (Italy): Regional reports and general correlation. Bolletino della Società Geologica Italiana, Volume speciale* (Vol. 2, pp. 1–24).

Stern, R. J., Reagan, M. K., Ishizuka, O., Ohara, Y., & Whattam, S. A. (2012). To understand subduction initiation, study forearc crust: To understand forearc crust, study ophiolites. *Lithosphere*, *4*(6), 469–483. https://doi.org/10.1130/L183.1

Topuz, G., Celik, O. F., Sengör, A. M. C., Altintas, I. E., Zack, T., Rolland, Y., & Barth, M. (2014). Jurassic ophiolite formation and emplacement as backstop to a subduction-accretion complex in northeast Turkey, the Refahiye ophiolite, and relation to the Balkan ophiolites. *American Journal of Science*, *313*(10), 1054–1087. https://doi.org/10.2475/10.2013.04

Topuz, G., Göçmengil, G., Rolland, Y., Çelik, Ö. F., Zack, T., & Schmitt, A. K. (2013). Jurassic accretionary complex and ophiolite from northeast Turkey: No evidence for the Cimmerian continental ribbon. *Geology*, *41*(2), 255–258. https://doi.org/10.1130/G33577.1

Topuz, G., Okay, A. I., Schwarz, W. H., Sunal, G., Altherr, R., & Kylander-Clark, A. R. (2017). A middle Permian ophiolite fragment in Late Triassic greenschist-to blueschist-facies rocks in NW Turkey: An earlier pulse of suprasubduction-zone ophiolite formation in the Tethyan belt. *Lithos*, *300–301*, 121–135.

Torsvik, T. H., & Cocks, L. R. M. (2017). *Earth history and palaeogeography*. Cambridge: Cambridge Univ. Press. https://doi.org/10.1017/9781316225523

Torsvik, T. H., Gül, M., Cronin, B. T., & Gürbüz, K. (2012). Phanerozoic polar wander, palaeogeography and dynamics. *Earth-Science Reviews*, *114*(3-4), 195–217. https://doi.org/10.1016/j.earscirev.2012.06.002

Torsvik, T. H., Steinberger, B., Gurnis, M., & Gaina, C. (2010). Plate tectonics and net lithosphere rotation over the past 150 My. *Earth and Planetary Science Letters*, *291*(1-4), 106–112. https://doi.org/10.1016/j.epsl.2009.12.055

Tremblay, A., Meshi, A., & Bédard, J. H. (2009). Oceanic core complexes and ancient oceanic lithosphere: Insights from Iapetan and Tethyan ophiolites (Canada and Albania). *Tectonophysics*, *473*(1-2), 36–52. https://doi.org/10.1016/j.tecto.2008.08.003

Tremblay, A., Meshi, A., Deschamps, T., Goulet, F., & Goulet, N. (2015). The Vardar zone as a suture for the Mirdita ophiolites, Albania: Constraints from the structural analysis of the Korabi-Pelagonia zone. *Tectonics*, *34*(2), 352–375. https://doi.org/10.1002/2014TC003807

Ustaömer, T., & Robertson, A. H. (1993). A Late Palaeozoic-Early Mesozoic marginal basin along the actives sourthern continental margin of Eurasia: Evidence from the central Pontides (Turkey) and adjacent regions. *Geological Journal*, *28*(3-4), 219–238. https://doi.org/10.1002/gj.3350280303

Ustaömer, T., & Robertson, A. H. (1999). Geochemical evidence used to test alternative plate tectonic models for pre-Upper Jurassic (Palaeotethyan) units in the Central Pontides, N Turkey. *Geological Journal*, *34*(1-2), 25–53. https://doi.org/10.1002/(SICI)1099-1034(199901/06)34:1/2%3C25::AID-GJ813%3E3.0.CO;2-C

Uysal, I., Ersoy, E. Y., Dilek, Y., Escayola, M., Sarıfakıoğlu, E., Saka, S., & Hirata, T. (2015). Depletion and refertilization of the Tethyan oceanic upper mantle as revealed by the early Jurassic Refahiye ophiolite, NE Anatolia—Turkey. *Gondwana Research*, *27*(2), 594–611.

van Hinsbergen, D. J. J., Langereis, C. G., & Meulenkamp, J. E. (2005). Revision of the timing, magnitude and distribution of Neogene rotations in the western Aegean region. *Tectonophysics*, *396*(1-2), 1–34. https://doi.org/10.1016/j.tecto.2004.10.001

van Hinsbergen, D. J. J., & Schmid, S. M. (2012). Map view restoration of Aegean-West Anatolian accretion and extension since the Eocene. *Tectonics*, *31*(5), TC5005. https://doi.org/10.1029/2012TC003132

van Hinsbergen, D. J. J., et al. (2015). Dynamics of intraoceanic subduction initiation: 2. Suprasubduction zone ophiolite formation and metamorphic sole exhumation in context of absolute plate motions. *Geochemistry, Geophysics, Geosystems*, *16*, 1753–1770. https://doi.org/10.1002/2015GC005746

van Hinsbergen, D. J. J., et al. (2016). Tectonic evolution and paleogeography of the Kırşehir Block and the Central Anatolian Ophiolites, Turkey. *Tectonics*, *35*(4), 983–1014. https://doi.org/10.1002/2015TC004018

Vissers, R. L. M., Van Hinsbergen, D. J. J., Meijer, P. T., & Piccardo, G. B. (2013). Kinematics of Jurassic ultra-slow spreading in the piemonte Ligurian ocean. *Earth and Planetary Science Letters*, *380*, 138–150. https://doi.org/10.1016/j.epsl.2013.08.033

Vissers, R. L. M., van Hinsbergen, D. J. J., Wilkinson, C. M., & Ganerød, M. (2017). Middle Jurassic shear zones at Cap de Creus (eastern Pyrenees, Spain): A record of pre-drift extension of the Piemonte–Ligurian Ocean? *Journal of the Geological Society*, *174*(2), 289–300. https://doi.org/10.1144/jgs2016-014

Wakabayashi, J., & Dilek, Y. (2003). What constitutes "emplacement" of an ophiolite?: Mechanisms and relationship to subduction initiation and formation of metamorphic soles. *Geological Society of London, Special Publication*, *218*(1), 427–447. https://doi.org/10.1144/GSL.SP.2003.218.01.22

Zachariadis, P. T. (2007). Ophiolites of the eastern Vardar Zone, N. Greece. PhD Thesis, Johannes Gutenberg-Universitat Mainz, pp. 221.

Zachariadou, S., & Dimitriadis, S. (1995). Aspects of the tectono-magmatic evolution of the Late Jurassic Guevgueli Complex, Macedonia, Greece. *Geological Society Greece Special Publication*, *4*, 143–147.

Zelic, M., Marroni, M., Pandolfi, L., & Trivić, B. (2010). Tectonic setting of the vardar suture zone (Dinaric-Hellenic Belt): The example of the Kopaonik area (Southern Serbia). *Ofioliti*, *35*(1), 49–69.

Zijderveld, J. D. A. (1967). A. C. demagnetization of rocks: Analysis of results. In D. W. Collinson, K. M. Creer, & S. K. Runcorn (Eds.), *Methods in Palaeomagnetism* (pp. 254–286). New York: Elsevier.